Observed relationships between Sudden Stratospheric Warmings and European climate extremes

Andrew D. King[1,2], Amy H. Butler[3], Martin Jucker[4,2], Nick O. Earl[1,5], and Irina Rudeva[1,6]

1. School of Earth Sciences, University of Melbourne, Melbourne, Victoria, Australia.

2. ARC Centre of Excellence for Climate Extremes, Australia.

3. CIRES/University of Colorado-Boulder and NOAA/Chemical Sciences Division, Boulder, Colorado, United States.

4. Climate Change Research Centre, University of New South Wales, Sydney, New South Wales, Australia.

5. Climate Futures, University of Tasmania, Hobart, Tasmania, Australia.

6. Shirshov Institute of Oceanology, Russian Academy of Sciences, Moscow, Russia

This is the author manuscript accepted for publication and has undergone full peer review but has not been through the copyediting, typesetting, pagination and proofreading process, which may lead to differences between this version and the Version of Record. Please cite this article as doi: 10.1029/2019JD030480

Corresponding author: Andrew King (andrew.king@unimelb.edu.au)

Key Points

- Using gridded observational surface data we find a link between SSWs and European climate means and extremes.
- Cooler average temperatures precede SSWs over much of Northern Europe but the intensity of cold extremes is greater after SSWs.
- Methodological design has a large effect on the apparent strength of relationship between SSWs and European climate.

Abstract

Sudden stratospheric warmings (SSWs) have been linked with anomalously cold temperatures at the surface in the mid-to-high latitudes of the Northern Hemisphere as climatological westerly winds in the stratosphere tend to weaken and turn easterly. However, previous studies have largely relied on reanalyses and model simulations to infer the role of SSWs on surface climate and SSW relationships with extremes have not been fully analysed. Here, we use observed daily gridded temperature and precipitation data over Europe to comprehensively examine the response of climate extremes to the occurrence of SSWs. We show that for much of Scandinavia, winters with SSWs are on average at least 1°C cooler, but the coldest day and night of winter is on average at least 2°C colder than in non-SSW winters. Anomalously high pressure over Scandinavia reduces precipitation on the northern Atlantic coast but increases overall rainfall and the number of wet days in southern Europe. In the 60 days after SSWs, cold extremes are more intense over Scandinavia with anomalously high pressure and drier conditions prevailing. Over Southern Europe there is a tendency towards lower pressure, increased precipitation and more wet days. The surface response in cold temperature extremes over northwest Europe to the 2018 SSW was stronger than observed for any SSW during 1979-2016. Our analysis shows that SSWs have an effect not only on mean climate, but also extremes over much of Europe. Only with carefully designed analyses are the relationships between SSWs and climate means and extremes detectable above synoptic-scale variability.

Plain Language Summary

Sudden stratospheric warmings (SSWs) are rapid warming events that occur tens of kilometres above the Earth's surface in the Northern Hemisphere. They are often associated with cold winter weather at the surface in the Northern Hemisphere, but previously the connection between SSWs and cold extremes has been made using reanalyses and models rather than observational data. We performed the first comprehensive analysis of the link between SSWs and climate extremes in Europe. We found that winters with SSWs are substantially colder than average in areas like Scandinavia. Below-average temperatures tend to precede SSW events, but the intensity of cold extremes, such as the coldest night of the month, tends to be strongest after the SSW event. Precipitation tends to decrease in northern Europe in winters with SSWs, but in Southern Europe the aftermath of an SSW is often associated with more precipitation and an above-average number of wet days. The 2018 SSW, for which the subsequent surface cold event was referred to as "The Beast from the East", exhibited stronger cold anomalies in extreme indices over northwest Europe than any SSW in the 1979-2016 period. Through this analysis we found a link between SSWs and European wintertime climate extremes.

1. Introduction

Sudden stratospheric warmings (SSWs) are extreme synoptic events in the winter stratosphere. They occur almost exclusively in the Northern Hemisphere, on average about once every two years. During these events the climatological pattern of strong westerly zonal winds in the middle atmosphere (10-50km above the surface) of the Northern Hemisphere high latitudes becomes disrupted as the stratospheric temperature rises rapidly and the upper-level winds become easterly. The causes of SSW events are still not fully understood, but two

likely possibilities include Rossby wave propagation from the troposphere into the stratosphere which disrupts the strong zonal circulation aloft (Matsuno, 1971; Polvani & Waugh, 2004), and internal resonance of the stratospheric polar vortex (Albers & Birner, 2014; Matthewman & Esler, 2011). SSWs are also often preceded by tropospheric blocking at high latitudes which is also thought to have an effect at higher altitudes (Martius et al., 2009; White et al., 2019), and probabilistic increases in SSW occurrence have been tied to teleconnections with the El Niño-Southern Oscillation (ENSO; Butler and Polvani 2011; Ineson and Scaife 2009; Polvani et al. 2017; Domeisen et al. 2019) and the Madden-Julian Oscillation (MJO; Garfinkel et al., 2012).

These SSW events are important, in part, because they have been associated with anomalous, high-impact, surface weather patterns in the Northern Hemisphere mid-latitudes (Baldwin & Dunkerton, 2001). The anomalous upper-level easterly winds can propagate down to the surface causing enhanced atmospheric blocking (Woollings et al., 2010). In some cases these SSW events and associated blocking have been linked with extreme cold temperatures and heavy snowfall in parts of Europe, such as the February 2018 cold spell dubbed “The Beast from the East” in the United Kingdom (e.g. BBC News, 2018). Additionally, drought-breaking precipitation in the Iberian peninsula was also linked with the February 2018 SSW event (Ayarzagüena et al., 2018).

Despite the strong influence SSW events have been shown to have on European weather, only one previous study, to the authors’ knowledge, examines SSW relationships with station data including a single extreme temperature index (Thompson et al., 2002). Previous work has largely relied on weather and climate models (e.g. Charlton-Perez et al., 2013; Tomassini

et al., 2012) and reanalyses (Butler et al., 2017; Kolstad et al., 2010; Lehtonen & Karpechko, 2016; Palmeiro et al., 2017) to investigate the tropospheric/surface responses to SSW events.

Few previous analyses have focussed on the relationships between SSWs and extremes, although several studies have used reanalyses to examine stratospheric polar vortex links to cold extremes (Kretschmer, Cohen, et al., 2018; Kretschmer, Coumou, et al., 2018). There are no previous studies that investigate the association between SSW events and climate extremes using indices such as those defined by the World Meteorological Organisation. This is despite the fact that there have been many analyses examining relationships between other modes of climate variability, such as ENSO (Grotjahn et al., 2016; King et al., 2014), or specific meteorological phenomena, such as atmospheric blocking (Brunner et al., 2017; Whan et al., 2016), and climate extreme indices across many regions of the world. European winter and springtime temperature extremes have been investigated for their relationships with the North Atlantic Oscillation (NAO) and atmospheric blocking (Brunner et al., 2017; Diao et al., 2015) with more frequent and intense cold winter extremes associated with negative NAO and surface blocking (Cattiaux et al., 2010; J. j.-M. Hirschi & Sinha, 2007).

To better understand the role of SSWs in European climate extremes a comprehensive observation-based study is needed to examine these relationships. There are many benefits to better constraining the observed relationships between SSWs and climate extremes, including improving our understanding of the surface response to SSW events with a view to potentially predicting the occurrence and severity of cold extremes at longer lead-times. In this study we use gridded observed climate data over Europe and a database of SSW cases to

investigate the relationship between SSWs and European temperature and precipitation extremes.

2. Data and Methods

Previous analyses have identified observed SSW events using reanalyses (Butler et al., 2017; Charlton & Polvani, 2007). These studies find generally good agreement between widely used reanalyses, except in surface-input reanalyses, such as the NOAA Twentieth Century Analysis (Compo et al., 2011), in the occurrence and timing of SSWs, especially in the satellite era (Gerber & Martineau, 2018). We focus on the 24 SSWs that occurred in the 1979-2016 period (Table 1) using the ERA-Interim reanalysis (Dee et al., 2011) as identified by Butler et al., (2017). Sensitivity testing of our analysis to the extended record of SSWs back to 1958 using the ERA-40 reanalysis (Uppala et al., 2005) produces broadly similar results (not shown).

For the analysis of European surface climate we used the European gridded dataset of observed temperature, precipitation and mean sea level pressure (MSLP) referred to as E-OBS (van den Besselaar et al., 2011; Haylock et al., 2008). This dataset covers the period 1950-2017 (E-OBS version 17.0) and includes daily gridded maximum temperature, minimum temperature, precipitation (including all precipitation types with no separation), and MSLP. The dataset was compiled through the interpolation of data from in situ stations across Europe onto a regular 0.5° grid for land-only locations, but there are locations and times for which there is missing data (shown in white areas on Figures throughout this study). This dataset has been evaluated extensively (e.g. van den Besselaar et al., 2011; Haylock et

al., 2008) and used in previous analyses of European climate for observational analyses (M. Hirschi et al., 2011; Manning et al., 2019) and model evaluation (e.g. Fischer et al., 2012). The newer E-OBS version 19.0 (Cornes et al., 2018) was used to contextualise the February 2018 SSW against the climatology of SSWs between 1979 and 2016. E-OBS version 19.0 was not used for the entire analysis as it is very different in design from previous versions, being an ensemble product at higher resolution, and has not been evaluated or analysed for trends (van der Schrier et al., 2013) to the extent that previous versions have been. However, a comparison of results between these datasets shows little difference (not shown). The use of a gridded dataset allows for a spatially complete or near-complete analysis, but the interpolation introduces some uncertainties which are larger where there are fewer station data available, such as in areas of Eastern Europe.

We extracted a set of mean and extreme climate indices (Table 2) from E-OBS (v17.0) for the 1979-2016 period. A selection of temperature and precipitation indices that are versatile in their calculation and comparison over different periods was chosen (as explained below). As such, the extreme indices largely represent the intensity of temperature and precipitation extremes. The extreme indices used here are similar to those proposed by the World Meteorological Organisation Expert Team on Climate Change Detection and Indices (Zhang et al., 2011). The modification to the indices used here is the calculation of the indices over moving 30-day windows rather than calendar months to account for differences in timing between SSWs.

Firstly, a climatology of all mean and extreme climate indices was compiled for the 1979-2016 period. Climatologies were calculated at every gridpoint for which data was available

throughout this period and for four larger regional-averages: the British Isles [11°W-2°E, 50°N-60°N], Southern Scandinavia [3°E-18°E, 57°N-64°N], Iberia [10°W-1°E, 36°N-44°N], and Eastern Europe [18°E-26°E, 40°N-50°N]. The climatologies were calculated for all indices for the cold season (defined as November-April, although the robustness of the analysis to the use of shorter timeframes was tested). The climatologies for mean indices were also calculated for each calendar date.

To examine the statistical significance of the differences in these indices between seasons with and without SSWs, the Wilcoxon rank-sum test was used to compare median-averages. A more commonly used student t-test could have been applied to compare the mean-averages of the temperature indices and MSLP, but would not have been suitable for examining differences in mean and extreme precipitation indices which are strongly non-Gaussian. Initially all the mean and extreme indices were compared between winters with and without SSWs, similar to comparisons made previously (e.g. Polvani et al., 2017). This technique allows for general comparisons to be made but does not account for the different timings of SSWs between seasons. In particular, SSWs have short predictability timescales (Tripathi et al., 2015) and other influences such as ENSO, which may affect SSW occurrence (Butler & Polvani, 2011) but also has a tropospheric teleconnection to Europe (Jiménez-Esteve & Domeisen, 2018) may be aliased into these comparisons. Thus, while the comparison of winters with and without SSWs is useful in framing the remainder of the analysis, this comparison may not clearly isolate the influence of SSWs on European climate.

To identify climatic changes around SSW events, a range of shorter timescales were investigated. For each SSW, anomalies in 30-day moving windows of maximum and

minimum temperature, precipitation and MSLP were calculated relative to climatologies computed for the same calendar day 30-day windows throughout the 1979-2016 period. These anomalies were then averaged across the 24 SSW events in the 1979-2016 period for each time window relative to the central date of the SSW. This method allows for the comparison of temperature, precipitation and MSLP anomalies between SSWs despite the occurrence of SSWs at different times within the cold season. The same method was applied to look at anomalous values of temperatures, precipitation and MSLP in 5-day and 11-day periods before and after SSWs. Consistency in the sign of anomalies relative to the SSW central date across the 24 cases of SSW events was also assessed through simply identifying the level of agreement in the sign of temperature, precipitation and MSLP anomalies in each windowed period at each gridbox.

The relationship between SSWs and extreme indices was investigated using a similar approach. For each SSW event, the extreme index (e.g. the coldest daily minimum temperature, TNn) was calculated from the relevant variable from the E-OBS dataset for 30-day windows anchored to the central SSW event date. For example, for the first SSW in the ERA-Interim series with a central date of 22nd February 1979 (Table 1), each extreme index was calculated for the 30-day period prior to that date, in this case 23rd January-21st February 1979. The anomalous value of each index was then calculated by subtracting the extreme index for that 30-day window with the mean-average for all other 30-day windows for the same time of year (i.e. in our example this would be all other 23rd January-21st February windows in the 1980-2016 period). The average of these anomalous values across the SSW events was then calculated. As for the mean indices, agreement was assessed by computing

the proportion of SSW events where the anomaly is of the same sign. The signal-to-noise in the SSW anomalies was also calculated as a measure of the significance of anomalies before and after SSWs and is described in Supplementary Text S1.

Windows of 30 days were used as this allows for the calculation of extreme indices, whereas 5- and 11-day windows are too short to produce meaningful and useful values of indices like TNn and TXn. The 30-day periods before (-30 days to -1 day), after (event date to +29 days), and the second month after (+30 days to +59 days) the SSW date were investigated, similar to Lehtonen & Karpechko, (2016) which examined surface responses to SSW events in ERA-Interim.

To better understand the relationships between SSWs and climate means and extremes we examined probability density functions of daily anomalies of maximum and minimum temperature in four regions as defined previously (British Isles, Southern Scandinavia, Iberia, and Eastern Europe) both in winters with and without SSWs, and in 30-day periods before and after SSWs. The median-average and 10^{th} and 90^{th} percentiles of anomalies in the pairs of distributions were compared.

Data for the daily NAO and Arctic Oscillation (AO) indices were downloaded from the National Oceanographic and Atmospheric Administration website (https://www.cpc.ncep.noaa.gov/products/precip/CWlink/daily_ao_index/teleconnections.shtml) and information on the methods for calculating these indices may be found on the website. Standardised daily NAO and AO anomalies were analysed for relationships with SSW events. The NAO and AO are strongly related to European climate variability (Baldwin

& Dunkerton, 2001; Scaife et al., 2008; Trigo et al., 2002). The NAO and AO have also been linked with SSW events whereby major SSWs are associated with negative NAO/AO conditions (i.e. weakening and equatorward displacement of westerly flow over the North Atlantic) in reanalyses and models (e.g. Haase et al., 2018). We examined the NAO and AO through plotting the daily evolution of anomalies across SSW events relative to the date of the SSW and by comparing statistical distributions of anomalies in 30-day windows before and after the SSW event date.

Significance testing on the skewness of the distributions of daily temperature and daily NAO values was undertaken for winters with and without SSWs and 30-day periods before and after SSW events. The significance of the skewness was estimated using the standard error which is approximated as $\sigma_s = \sqrt{\frac{6}{N_i}}$, where N_i is the effective number of degrees of freedom (Tamarin-Brodsky et al., 2019). The sample size is reduced by a factor of seven in all cases as an estimate of the effective number of degrees of freedom based on a typical atmospheric decorrelation timescale (Tamarin-Brodsky et al., 2019). Skewness is estimated to be statistically significant if the absolute value of skewness is greater than $2\sigma_s$ (Holzer, 1996). The overall distributions were compared for similarity using a Kolmogorov-Smirnov test and deemed significantly different if there was less than 5% likelihood of the two samples being taken from the same overall population. The differences in 10^{th}, 50^{th} and 90^{th} percentiles between temperature distributions were tested for significance by bootstrap resampling 50% of seasons (in the case of SSW versus non-SSW winters) or SSW seasons (in the case of periods before SSWs versus periods after SSWs) 1000 times and recalculating the respective

percentiles. If in more than 97.5% of the bootstrapped subsamples the difference between the percentile of interest was the same sign then the difference at that percentile was considered statistically significant at the 5% level.

SSWs can be classified in different categories depending on their evolution and structure. Two broad classes, referred to as “split” and “displacement” have been identified, and SSW events have been catalogued (Charlton & Polvani, 2007; Kuttippurath & Nikulin, 2012). Previous research has suggested that different SSW types may have different impacts on surface climate over Europe (Mitchell et al., 2013), although the differences may be largely non-significant (Lehtonen & Karpechko, 2016). We used the event classifications based on Lehtonen & Karpechko (2016), which covered the period until 2010 and followed earlier studies (Charlton & Polvani, 2007; Cohen & Jones, 2011; Kuttippurath & Nikulin, 2012) with the 2013 SSW classified following Coy & Pawson, (2015). Note that these classifications may be sensitive to methodology. Anomalies in mean and extreme indices were compared between winters with split SSWs and winters with displaced SSWs.

No detrending was applied in this analysis as previous work (van der Schrier et al., 2013) has identified a winter warming trend that is dominated by noise, even on a continent-wide average scale. As the variability is much larger than the trends, especially on the gridbox scale, we assume that the influence of anthropogenic warming plays little role in our results.

3. Results

3.1. SSW winters versus non-SSW winters

Firstly, a comparison of mean and extreme climate indices was made between cool seasons (November-April) with and without SSW events. Average minimum temperatures (TN) are cooler across the majority of the European continent in winters with SSW events compared to winters without SSWs (Figure 1a). The largest differences are in land areas around the Baltic Sea with much of Finland, the Baltic states, and northwestern Russia more than 1°C colder on average in cool seasons with SSW events than those without. The differences are significant over most of Scandinavia and areas of Eastern Europe, but also in the Alpine region and parts of Britain where the average difference in minimum temperatures is comparatively small at around 0.5°C.

In cool seasons with SSW events, the coldest minimum temperature (TNn) is substantially lower over most of northern Europe, especially in Norway and Sweden where on average the coldest minimum is more than 2.5°C colder in winters with SSWs than those without (Figure 1b). In general, the pattern of differences in TNn between winters with and without SSWs is similar to the pattern of TN differences, but with greater spatial heterogeneity due to the noisiness of extreme temperatures relative to average temperatures.

The differences in average maximum temperatures (TX; Figure 1c) and the coldest maximum temperature (TXn; Figure 1d) between winters with and without SSWs are broadly similar to those found for TN and TNn. The same region of Norway and Sweden that experiences substantially colder TNn values in winters with SSWs, also experiences much colder TXn values in winters with SSWs versus winters without SSWs.

The use of shorter cool seasons (December-March instead of November-April) and the reassignment of cool seasons with SSWs only in March as non-SSW winters makes little difference to the results (not shown). The patterns of temperature differences between winters with and without SSW events appear to be robust to such choices.

Cool seasons with SSW events tend to be substantially and significantly drier over Ireland, Scotland and western coasts of Norway than seasons without an SSW event (Figure 2a). Over most of southern Europe, cool seasons with SSWs tend to be slightly wetter than those without but the differences are largely non-significant. For the wettest day of the cool season (Rx1day; Figure 2b) there is little pattern and a high degree of spatial heterogeneity to the differences between seasons with and without SSWs. However, over western Scotland and the Norwegian coast there are significant decreases in Rx1day in cool seasons with SSWs compared to cool seasons without. The difference in the number of wet days between seasons with and without SSWs (Figure 2c) largely follows the pattern of differences for average precipitation. There are more wet days over southern Europe and fewer wet days on Atlantic coasts of northern Europe in winters with SSWs compared to winters without.

On average the MSLP in winters with SSWs is higher over Scandinavia and lower over southern Europe compared to winters without SSWs (Figure 2d). These differences are significant over northern Scandinavia and southeastern Europe and broadly reflect the difference in precipitation between winters with and without SSWs (Figure 2a).

3.2.Evolution of climate anomalies before and after SSWs

The substantial and significant anomalies in climatic conditions over much of Europe in cool seasons with SSWs motivated further analysis. The temporal evolution of climate anomalies relative to the SSW central dates was subsequently investigated. Average minimum and maximum temperatures in the month before an SSW event are anomalously cool over much of Europe, especially in the east (Figure 3). After the SSW occurs the average anomalies weaken over most of the continent. However, in very few locations, even prior to the SSW when the anomalies are strongest, is consistency found in the sign of the temperature anomaly indicating high variability in the evolution of temperature anomalies between events. This pattern of cooler anomalies ahead of the SSW event has been found previously using ERA-Interim (Lehtonen & Karpechko, 2016) and the similarity extends to the location and magnitude of the coolest temperature anomalies in Europe to the east of the Baltic states.

Both before and after SSW events there is a tendency for drier conditions to prevail on average over Atlantic coasts of northern Europe (Figure 4) with a slight weakening of the dry anomaly after the SSW compared to before the event. There are on average wetter conditions over southern Europe, especially the Iberian peninsula, but there is high variability in anomalies between events. Displaying these anomalies in terms of a percentage of average precipitation at each location (Figure S1) highlights the substantial wet anomalies in Spain especially, although the dry anomalies after SSW events in relatively wet regions such as Norway, Scotland and Ireland, remain clear.

The precipitation anomaly composites align with the observed MSLP anomalies before and after SSWs (Figure 4). In the period before an SSW, higher pressure over northern Europe is more likely, albeit with low agreement between SSWs aside from over northern Britain. In

the month after an SSW when wetter-than-average conditions are more likely over southern Europe, there is also a tendency for lower MSLP with relatively high agreement between individual SSW events. This pattern weakens in the second month after an SSW. Persistent high pressure anomalies at mid-to-high-latitudes (i.e. blocking patterns) have been found to precede SSWs previously and it has been mooted that they contribute to their formation (Martius et al., 2009).

In addition to examining observed surface climate anomalies in 30-day windows before and after SSWs, shorter 11-day (Figures S2, S3) and 5-day windows (Figure S4) were also used. These demonstrate a similar pattern of anomalies found as in the 30-day windows, but with a low degree of consistency in the sign of anomalies between SSW phases indicative of large synoptic-scale variability between events.

Climate extreme indices in many regions exhibit a stronger and clearer relationship with SSW events than was found in mean climate variables. The coldest daily minimum temperature (TNn) and coldest daily maximum temperature (TXn) in 30-day windows before and after SSWs is on average anomalously cool especially over northern and eastern areas of Europe (Figure 5). Unlike for mean temperatures where there are larger cool anomalies before the SSW event, for TNn and TXn the greatest cold anomalies, and consistency in these anomalies across events, is after the SSW occurs. In areas of Scandinavia and the Baltic states, where on average minimum temperatures may be 1-2°C cooler in the first and second month after an SSW, the coldest minimum is on average 3-5°C colder than normal. The average TNn and TXn anomalies across the 24 SSWs generally follow similar spatial and temporal patterns in Europe through the SSW events.

Comparatively, the extreme precipitation indices studied here show less of a clear SSW relationship (Figure 6). On average there are more wet days and higher values of Rx1day (the wettest day of the period) in France and Iberia immediately after the SSW event occurs. There are concurrent dry anomalies in these indices on the Atlantic coast of northern Europe, but in general the signal is not consistent.

3.3.Daily temperature distributions before and after SSWs

Our results point to relationships between SSWs and both mean and extreme temperatures. However, the clearest indication of a relationship is found when considering temperature anomalies through entire cool seasons with and without SSWs (Figure 1; noting that this could be related to other climate influences) and when examining extended windows of 30-days before and after SSW events (Figure 3,5). To explore the SSW relationship with mean and extreme temperatures further we aggregated the daily anomalies (from a calendar-date dependent climatology) across the entire cool seasons for the four regional-averages discussed previously: the British Isles, Southern Scandinavia, Iberia, and Eastern Europe. We firstly compared the distributions of daily minimum and maximum temperature anomalies between cool seasons with and without SSWs (Figures S6, S7) and we found substantial differences in not only the median-average values, but also in the shapes of the distributions including in the skewness.

An intriguing result noted above was that the coolest anomalies in average temperatures are typically before the SSW event occurs (Figure 3) whereas the coldest extremes are more intense after the SSW event has occurred (Figure 5). To better understand this divergence in

mean and extreme temperature relationships with SSW events, we compared distributions of daily TN and TX anomalies in the 30-day windows before and after SSW events occur in the same four regions (Figure 7, S10). In Southern Scandinavia, Iberia and Eastern Europe average minimum temperature anomalies are higher in the aftermath of the SSW, but the differences in the medians are not statistically significant. In both Southern Scandinavia and Eastern Europe, however, the differences in 10^{th} percentile minimum temperature anomalies are on average much smaller and these differences are not statistically significant due to large uncertainty in the distribution. In Southern Scandinavia and Eastern Europe, the distributions are more negatively skewed in the 30-day window after the SSW than the 30-day window before, such that the difference in cold extremes is smaller than the average. In Eastern Europe, the negative skewness is statistically significant after the SSW, but not before. The maximum temperature distributions appear to shift in the mean more than change in higher order characteristics such as variability and skewness (Figure S8).

We examined the temporal evolution of observed daily standardised NAO and AO values before and after SSW events in addition to the distributions of NAO and AO in 30-day windows before and after SSW events (Figure 8). In the second month after the SSW central date there is a slight tendency towards more negative NAO conditions (Domeisen, 2019) and the distribution is significantly negatively skewed, reflective of the MSLP anomalies found in the "decay" period (31-60 days post-central SSW date) after SSWs previously (Lehtonen & Karpechko, 2016), but the signal is weak. The AO also tends to be negative after SSW events (Baldwin & Dunkerton, 2001), although with significant variability between events. There is a slight difference between the NAO and AO average anomalies before and after the SSW

central date despite the strong relationship between the NAO and AO (e.g. Cohen & Barlow, 2005).

3.4. The SSW of February 2018

The February 2018 SSW received a large amount of attention from the public as it was associated with extreme cold and snow across northwest Europe. This event was examined by comparing the associated 2018 European climate anomalies with those from the climatology based on the 24 SSWs between 1979 and 2016. The 30-day period prior to the 2018 SSW was associated with both warmer average (not shown) and extreme temperatures (Figure 9) than seen on average for periods prior to other SSWs (Figures 3, 5). However, in the two months after the SSW the extreme temperature indices, TNn and TXn, show very large cold anomalies (Figure 9) which are considerably stronger than those in the average minimum and maximum temperatures (not shown). For southern Britain especially (Met Office, 2018), the coldest daytime maximum temperatures in the first and second month after the February 2018 SSW were anomalously colder than those observed in the aftermath of all 24 SSWs in the 1979-2016 period.

The precipitation anomalies before and after the SSW of 2018 (Figure 10) broadly reflect the average anomalies associated with SSWs in the climatology (Figure 4). There were record anomalous wet conditions relative to other SSWs, associated with lower than normal MSLP after the SSW of 2018 across parts of the Mediterranean (Figure 10; B. Ayarzagüena et al., 2018). Interestingly, and unusually, the much colder temperatures in parts of England occurred in 30-day windows with higher precipitation than normal as cold fronts brought late

winter heavy snow (Met Office, 2018). The anomalous easterly flow over northern Europe after the SSW of 2018 is evident in the MSLP anomaly maps (Figure 10) which are also broadly similar to the anomalies often associated with SSWs (Figure 4).

4. Discussion

Our study finds that there is a link between SSW events and European surface climate using observational data. To the authors' knowledge, this is the first study to use gridded observed data, as opposed to reanalyses or model simulations, in the assessment of the surface climate response across Europe to SSWs, and also the first study to examine the relationship between SSWs and climate extreme indices. These indices (Table 2) are similar to those used by the WMO to represent climate extremes and they are relevant to the impacts of extreme weather.

Our analysis reveals that colder average temperatures tend to occur prior to SSWs while the coldest extremes occur more often after SSWs. The difference in SSW relationships with mean and extreme temperatures is related to changes in the statistical distributions of daily temperatures before and after SSWs. This result highlights the need for extensive model analysis of surface climate extremes after SSWs to understand the processes driving this difference and to determine the predictability of extreme temperatures following SSW events. It is also intriguing that the mean and extreme precipitation indices and the pressure anomalies before and after SSWs do not follow a comparable evolution to the changes seen in the extreme temperature indices. This is consistent with the hypothesis that average changes in weather patterns before and after SSWs are weak, but that at some point in the first and second month after an SSW there is an increased likelihood of a cold snap.

Using gridded observational datasets to examine teleconnections between climate modes and phenomena and surface climate offers many opportunities, including the possibility of evaluating performance of reanalyses and models. Some of the relationships we have found between SSWs and mean temperatures and MSLP closely replicate those produced using ERA-Interim over the European continent (Lehtonen & Karpechko, 2016). This is despite methodological differences between these studies, particularly in the time period of analysis. Our findings give confidence that the ERA-Interim reanalysis is performing reasonably in this regard and suggests that it may be used for investigating mean surface climate responses to SSWs, although the purpose of this study was not to evaluate reanalyses. In addition to evaluation of reanalyses, the observed relationships between SSWs and European surface climate means and extremes found here may be used as the basis for evaluation of models used to examine surface effects of SSWs.

It has been suggested that there are precursors to SSW events that lend themselves to predictability of SSWs on multi-week timescales (Jucker & Reichler, 2018; Karpechko et al., 2018; Scaife et al., 2016). Given the observed relationships between SSWs and climate extremes, especially cold temperature extremes over Northern Europe in the two months after an SSW event, predictability of SSWs may also result in predictability of temperature extremes on sub-seasonal to seasonal timescales.

One limitation of our analysis is the sample size of 24 SSW events in the 1979-2016 period. As discussed previously, a longer 1958-2016 window could have been used by merging SSWs found using the ERA-40 dataset with those in ERA-Interim to obtain 37 cases. Some analysis based on this extended dataset produced similar results to those for the 1979-2016

period alone (not shown). However, the earlier period of E-OBS product (which extends back to 1950) has greater uncertainties as fewer *in situ* weather stations are available for that time (van der Schrier et al., 2013). Also, use of a longer period of study would have necessitated the application of a detrending to the temperature data and the choice of detrending itself would likely influence the results. As additional SSWs occur the consistency of the climate response may be compared with the findings of this work. Our analysis of the February 2018 SSW found some broad similarity in the temperature and precipitation anomalies before and after the SSW as seen across the climatology of the previous 24 SSWs.

Previous work has suggested that split- and displacement-type SSW events, which exhibit some different characteristics in many upper-level atmospheric features, could have different impacts on surface climate (Lehtonen & Karpechko, 2016; Mitchell et al., 2013), though long model simulations show little significant difference in the surface climate response (Jucker, 2016; Maycock & Hitchcock, 2015). Given the sample size of observed SSWs in our analysis, a full analysis of these differences using observational data is not robust. However, a cursory examination comparing the differences in observed temperature, precipitation and MSLP for split and displacement SSW events and non-SSW cool seasons was undertaken (Figures S8-S11). In general terms, the pattern of average differences in the temperature indices for split and displacement SSW cool seasons relative to non-SSW seasons is similar. For precipitation and MSLP, greater differences exist such that split SSWs tend to be associated with lower MSLP and greater precipitation over southwest Europe than displacement SSWs. This result is consistent with the work of Mitchell et al., (2013).

An important finding of our study is the dependence of results on the analysis of specific timescales. Examination of entire cool seasons and 30-day windows before and after SSWs yields substantial relationships between SSWs and climate means and extremes. However, the use of shorter timescales, such as 5-day and 11-day windows also analysed as part of this study, washes out the relationship due to reduced sample sizes. A further indication of this is shown Figure S13 where we plotted the evolution of average daily minimum temperature anomalies across the 24 SSW events before and after the SSW in the four regions studied previously. The average anomalies on any given date relative to an SSW are near-zero and the spread across the 24 SSWs (indicated by the interquartile range and 10^{th}-90^{th} percentile range) is substantial. This suggests substantial synoptic-scale variability limits our detection of a signal related to SSWs on short timescales.

Our study finds significant and substantial relationships between SSWs and climate extremes, but because the timing of cold extremes varies so much between individual SSWs, choices in the analysis inevitably dictate how strong the relationship appears to be. As SSWs either occur or do not occur, some statistical techniques such as correlation and regression analysis are not suitable either and there is likely some dependence in our results on the choice of SSW definitions. Thus, the design of analyses examining SSWs and climate extremes requires a different approach to studies which have examined relationships between other types of weather or climate variability, such as ENSO, and extremes. Any analysis of SSWs and climate extremes requires careful methodological design that allows for responses at differing lags between SSWs.

There is great interest in how European climate has already changed and may continue to change in a warmer world at the Paris Agreement global warming targets or higher (Beniston et al., 2007; Christidis & Stott, 2019; King & Karoly, 2017; Vautard et al., 2014). Given the strong relationships found here between SSWs and both mean and extreme climate indices at the surface, any projected changes in the frequency or intensity of SSWs, for which there is great uncertainty (Ayarzagüena et al., 2018; Kang & Tziperman, 2017), or their teleconnections to surface climate, would need to be well captured in order for robust wintertime climate projections for Europe.

Finally, Europe was chosen as the study region for this analysis due to the availability of a daily gridded dataset that exists over a long period and has had extensive work undertaken to ensure it is a high-quality product (van den Besselaar et al., 2011; Haylock et al., 2008; van der Schrier et al., 2013). Comparable studies could be performed for other regions where reanalyses suggest an SSW teleconnection with surface climate exists, such as North America, using *in situ* observations or daily gridded temperature and precipitation datasets.

5. Conclusions

Our study examines relationships between SSWs and mean and extreme surface climate conditions in Europe using observational data. We have found strong relationships between the occurrence of SSWs and anomalous mean and extreme climate conditions. Cool seasons with SSWs are substantially colder and drier than average over Northern Europe while in Southwestern Europe, wetter conditions are more likely. Anomalously cool conditions occur prior to SSW events over Northern Europe with monthly-average temperatures becoming less

anomalous in the aftermath of an SSW. In contrast, the coldest day and night in the months following an SSW are on average 3-5°C colder than normal over much of the north of the continent. The difference in the relationship between SSWs and average and extreme temperatures appears to be related to greater negative skewness in the daily temperature distributions in cool seasons with SSWs and in the aftermath of SSW events. The lagged response of cold extremes to SSW events suggests there should be predictability for cold extreme indices.

Our results point to a strong observed teleconnection between SSW events and European surface climate that has been found previously in studies using reanalyses and models. However, the timing of the response of surface extremes relative to SSWs varies greatly between events, such that the relationship is more nuanced than that often portrayed in the media.

Further analyses directly evaluating models and reanalyses against observational data for SSW-surface climate teleconnections and performing comparative studies for other regions are proposed.

Data Availability

All observational datasets used in this analysis are available online. The E-OBS dataset of European gridded daily observations is available from https://www.ecad.eu/download/ensembles/download.php. The daily NAO data is available from https://www.cpc.ncep.noaa.gov/products/precip/CWlink/pna/nao.shtml and the daily

NAM data is available from

https://www.cpc.ncep.noaa.gov/products/precip/CWlink/daily_ao_index/ao.shtml.

Acknowledgements

We acknowledge the E-OBS dataset from the EU-FP6 project ENSEMBLES (http://ensembles-eu.metoffice.com) and the data providers in the ECA&D project (http://www.ecad.eu). Andrew D. King was funded by the Australian Research Council (ARC) (DE180100638). Martin Jucker acknowledges support from an ARC grant (FL150100035) and the ARC Centre of Excellence for Climate Extremes (CE170100023). Irina Rudeva was supported by an ARC grant (DP160101997) and by a project funded by the Ministry of Science and Education of Russian Federation No. 14.616.21.0102 (ID RFMEFI61618X0102).

References

Albers, J. R., & Birner, T. (2014). Vortex Preconditioning due to Planetary and Gravity Waves prior to Sudden Stratospheric Warmings. *Journal of the Atmospheric Sciences*, *71*(11), 4028–4054. https://doi.org/10.1175/JAS-D-14-0026.1

Ayarzagüena, B., Barriopedro, D., Garrido-Perez, J. M., Abalos, M., Cámara, A., García-Herrera, R., … Ordóñez, C. (2018). Stratospheric Connection to the Abrupt End of the 2016/2017 Iberian Drought. *Geophysical Research Letters*, *45*(22), 12,639-12,646. https://doi.org/10.1029/2018GL079802

Ayarzagüena, Blanca, Polvani, L. M., Langematz, U., Akiyoshi, H., Bekki, S., Butchart, N., … Zeng, G. (2018). No robust evidence of future changes in major stratospheric sudden

warmings: a multi-model assessment from CCMI. *Atmospheric Chemistry and Physics*, *18*(15), 11277–11287. https://doi.org/10.5194/acp-18-11277-2018

Baldwin, M. P., & Dunkerton, T. J. (2001). Stratospheric harbingers of anomalous weather regimes. *Science (New York, N.Y.)*, *294*(5542), 581–4. https://doi.org/10.1126/science.1063315

BBC News. (2018). Europe freezes as "Beast from the East" arrives - BBC News. Retrieved January 26, 2019, from https://www.bbc.com/news/world-europe-43218229

Beniston, M., Stephenson, D. B., Christensen, O. B., Ferro, C. A. T., Frei, C., Goyette, S., … Woth, K. (2007). Future extreme events in European climate: an exploration of regional climate model projections. *Climatic Change*, *81*(S1), 71–95. https://doi.org/10.1007/s10584-006-9226-z

van den Besselaar, E. J. M., Haylock, M. R., van der Schrier, G., & Klein Tank, A. M. G. (2011). A European daily high-resolution observational gridded data set of sea level pressure. *Journal of Geophysical Research*, *116*(D11), D11110. https://doi.org/10.1029/2010JD015468

Brunner, L., Hegerl, G. C., & Steiner, A. K. (2017). Connecting Atmospheric Blocking to European Temperature Extremes in Spring. *Journal of Climate*, *30*(2), 585–594. https://doi.org/10.1175/JCLI-D-16-0518.1

Butler, A. H., & Polvani, L. M. (2011). El Niño, La Niña, and stratospheric sudden warmings: A reevaluation in light of the observational record. *Geophysical Research Letters*, *38*(13), n/a-n/a. https://doi.org/10.1029/2011GL048084

Butler, A. H., Sjoberg, J. P., Seidel, D. J., & Rosenlof, K. H. (2017). A sudden stratospheric warming compendium. *Earth System Science Data*, *9*(1), 63–76. https://doi.org/10.5194/essd-9-63-2017

Cattiaux, J., Vautard, R., Cassou, C., Yiou, P., Masson-Delmotte, V., & Codron, F. (2010). Winter 2010 in Europe: A cold extreme in a warming climate. *Geophysical Research Letters*, *37*(20), n/a-n/a. https://doi.org/10.1029/2010GL044613

Charlton-Perez, A. J., Baldwin, M. P., Birner, T., Black, R. X., Butler, A. H., Calvo, N., … Watanabe, S. (2013). On the lack of stratospheric dynamical variability in low-top versions of the CMIP5 models. *Journal of Geophysical Research: Atmospheres*, *118*(6), 2494–2505. https://doi.org/10.1002/jgrd.50125

Charlton, A. J., & Polvani, L. M. (2007). A New Look at Stratospheric Sudden Warmings. Part I: Climatology and Modeling Benchmarks. *Journal of Climate*, *20*(3), 449–469. https://doi.org/10.1175/JCLI3996.1

Christidis, N., & Stott, P. A. (2019). The Extremely Cold Start of the Spring of 2018 in the United Kingdom. *Bulletin of the American Meteorological Society*, Accepted.

Cohen, J., & Barlow, M. (2005). The NAO, the AO, and Global Warming: How Closely Related? *Journal of Climate*, *18*(21), 4498–4513. https://doi.org/10.1175/JCLI3530.1

Cohen, J., & Jones, J. (2011). Tropospheric Precursors and Stratospheric Warmings. *Journal of Climate*, *24*(24), 6562–6572. https://doi.org/10.1175/2011JCLI4160.1

Compo, G. P., Whitaker, J. S., Sardeshmukh, P. D., Matsui, N., Allan, R. J., Yin, X., …

Worley, S. J. (2011). The Twentieth Century Reanalysis Project. *Quarterly Journal of the Royal Meteorological Society*, *137*(654), 1–28. https://doi.org/10.1002/qj.776

Cornes, R. C., van der Schrier, G., van den Besselaar, E. J. M., & Jones, P. D. (2018). An Ensemble Version of the E-OBS Temperature and Precipitation Data Sets. *Journal of Geophysical Research: Atmospheres*, *123*(17), 9391–9409. https://doi.org/10.1029/2017JD028200

Coy, L., & Pawson, S. (2015). The Major Stratospheric Sudden Warming of January 2013: Analyses and Forecasts in the GEOS-5 Data Assimilation System. *Monthly Weather Review*, *143*(2), 491–510. https://doi.org/10.1175/MWR-D-14-00023.1

Dee, D. P., Uppala, S. M., Simmons, A. J., Berrisford, P., Poli, P., Kobayashi, S., … Vitart, F. (2011). The ERA-Interim reanalysis: configuration and performance of the data assimilation system. *Quarterly Journal of the Royal Meteorological Society*, *137*(656), 553–597. https://doi.org/10.1002/qj.828

Diao, Y., Xie, S.-P., & Luo, D. (2015). Asymmetry of Winter European Surface Air Temperature Extremes and the North Atlantic Oscillation. *Journal of Climate*, *28*(2), 517–530. https://doi.org/10.1175/JCLI-D-13-00642.1

Domeisen, D. I. V. (2019). Estimating the Frequency of Sudden Stratospheric Warming Events From Surface Observations of the North Atlantic Oscillation. *Journal of Geophysical Research: Atmospheres*, *124*(6), 3180–3194. https://doi.org/10.1029/2018JD030077

Domeisen, D. I. V., Garfinkel, C. I., & Butler, A. H. (2019). The Teleconnection of El Niño

Southern Oscillation to the Stratosphere. *Reviews of Geophysics*. https://doi.org/10.1029/2018RG000596

Fischer, E. M., Rajczak, J., & Schär, C. (2012). Changes in European summer temperature variability revisited. *Geophysical Research Letters, 39*(19), n/a-n/a. https://doi.org/10.1029/2012GL052730

Garfinkel, C. I., Feldstein, S. B., Waugh, D. W., Yoo, C., & Lee, S. (2012). Observed connection between stratospheric sudden warmings and the Madden-Julian Oscillation. *Geophysical Research Letters, 39*(18). https://doi.org/10.1029/2012GL053144

Gerber, E. P., & Martineau, P. (2018). Quantifying the variability of the annular modes: reanalysis uncertainty vs. sampling uncertainty. *Atmospheric Chemistry and Physics*, *18*(23), 17099–17117. https://doi.org/10.5194/acp-18-17099-2018

Grotjahn, R., Black, R., Leung, R., Wehner, M. F., Barlow, M., Bosilovich, M., … Prabhat. (2016). North American extreme temperature events and related large scale meteorological patterns: a review of statistical methods, dynamics, modeling, and trends. *Climate Dynamics*, *46*(3–4), 1151–1184. https://doi.org/10.1007/s00382-015-2638-6

Haase, S., Matthes, K., Latif, M., & Omrani, N.-E. (2018). The Importance of a Properly Represented Stratosphere for Northern Hemisphere Surface Variability in the Atmosphere and the Ocean. *Journal of Climate*, *31*(20), 8481–8497. https://doi.org/10.1175/JCLI-D-17-0520.1

Haylock, M. R., Hofstra, N., Klein Tank, A. M. G., Klok, E. J., Jones, P. D., & New, M. (2008). A European daily high-resolution gridded data set of surface temperature and

precipitation for 1950–2006. *Journal of Geophysical Research*, *113*(D20), D20119. https://doi.org/10.1029/2008JD010201

Hirschi, J. j.-M., & Sinha, B. (2007). Negative NAO and cold Eurasian winters: how exceptional was the winter of 1962/1963? *Weather*, *62*(2). Retrieved from https://rmets.onlinelibrary.wiley.com/doi/pdf/10.1002/wea.34

Hirschi, M., Seneviratne, S. I., Alexandrov, V., Boberg, F., Boroneant, C., Christensen, O. B., … Stepanek, P. (2011). Observational evidence for soil-moisture impact on hot extremes in southeastern Europe. *Nature Geoscience*, *4*(1), 17–21. https://doi.org/10.1038/ngeo1032

Holzer, M. (1996). Asymmetric Geopotential Height Fluctuations from Symmetric Winds. *Journal of the Atmospheric Sciences*, *53*(10), 1361–1379. https://doi.org/10.1175/1520-0469(1996)053<1361:AGHFFS>2.0.CO;2

Ineson, S., & Scaife, A. A. (2009). The role of the stratosphere in the European climate response to El Niño. *Nature Geoscience*, *2*(1), 32–36. https://doi.org/10.1038/ngeo381

Jiménez-Esteve, B., & Domeisen, D. I. V. (2018). The Tropospheric Pathway of the ENSO–North Atlantic Teleconnection. *Journal of Climate*, *31*(11), 4563–4584. https://doi.org/10.1175/JCLI-D-17-0716.1

Jucker, M. (2016). Are Sudden Stratospheric Warmings Generic? Insights from an Idealized GCM. *Journal of the Atmospheric Sciences*, *73*(12), 5061–5080. https://doi.org/10.1175/JAS-D-15-0353.1

Jucker, M., & Reichler, T. (2018). Dynamical Precursors for Statistical Prediction of Stratospheric Sudden Warming Events. *Geophysical Research Letters*, *45*(23), 2018GL080691. https://doi.org/10.1029/2018GL080691

Kang, W., & Tziperman, E. (2017). More Frequent Sudden Stratospheric Warming Events due to Enhanced MJO Forcing Expected in a Warmer Climate. *Journal of Climate*, *30*(21), 8727–8743. https://doi.org/10.1175/JCLI-D-17-0044.1

Karpechko, A. Y., Charlton-Perez, A., Balmaseda, M., Tyrrell, N., & Vitart, F. (2018). Predicting Sudden Stratospheric Warming 2018 and Its Climate Impacts With a Multimodel Ensemble. *Geophysical Research Letters*, *45*(24), 13,538-13,546. https://doi.org/10.1029/2018GL081091

King, A. D., & Karoly, D. (2017). Climate extremes in Europe at 1.5 and 2 degrees of global warming. *Environmental Research Letters*. https://doi.org/10.1088/1748-9326/aa8e2c

King, A. D., Klingaman, N. P., Alexander, L. V., Donat, M. G., Jourdain, N. C., & Maher, P. (2014). Extreme Rainfall Variability in Australia: Patterns, Drivers, and Predictability*. *Journal of Climate*, *27*(15), 6035–6050. https://doi.org/10.1175/JCLI-D-13-00715.1

Kolstad, E. W., Breiteig, T., & Scaife, A. A. (2010). The association between stratospheric weak polar vortex events and cold air outbreaks in the Northern Hemisphere. *Quarterly Journal of the Royal Meteorological Society*, *136*(649), 886–893. https://doi.org/10.1002/qj.620

Kretschmer, M., Coumou, D., Agel, L., Barlow, M., Tziperman, E., & Cohen, J. (2018). More-Persistent Weak Stratospheric Polar Vortex States Linked to Cold Extremes.

Bulletin of the American Meteorological Society, *99*(1), 49–60. https://doi.org/10.1175/BAMS-D-16-0259.1

Kretschmer, M., Cohen, J., Matthias, V., Runge, J., & Coumou, D. (2018). The different stratospheric influence on cold-extremes in Eurasia and North America. *Npj Climate and Atmospheric Science*, *1*(1), 44. https://doi.org/10.1038/s41612-018-0054-4

Kuttippurath, J., & Nikulin, G. (2012). A comparative study of the major sudden stratospheric warmings in the Arctic winters 2003/2004–2009/2010. *Atmospheric Chemistry and Physics*, *12*(17), 8115–8129. https://doi.org/10.5194/acp-12-8115-2012

Lehtonen, I., & Karpechko, A. Y. (2016). Observed and modeled tropospheric cold anomalies associated with sudden stratospheric warmings. *Journal of Geophysical Research: Atmospheres*, *121*(4), 1591–1610. https://doi.org/10.1002/2015JD023860

Manning, C., Widmann, M., Bevacqua, E., Van Loon, A. F., Maraun, D., & Vrac, M. (2019). Increased probability of compound long-duration dry & hot events in Europe during summer (1950-2013). *Environmental Research Letters*. https://doi.org/10.1088/1748-9326/ab23bf

Martius, O., Polvani, L. M., & Davies, H. C. (2009). Blocking precursors to stratospheric sudden warming events. *Geophysical Research Letters*, *36*(14), L14806. https://doi.org/10.1029/2009GL038776

Matsuno, T. (1971). A Dynamical Model of the Stratospheric Sudden Warming. *Journal of the Atmospheric Sciences*, *28*(8), 1479–1494. https://doi.org/10.1175/1520-

0469(1971)028<1479:ADMOTS>2.0.CO;2

Matthewman, N. J., & Esler, J. G. (2011). Stratospheric Sudden Warmings as Self-Tuning Resonances. Part I: Vortex Splitting Events. *Journal of the Atmospheric Sciences*, *68*(11), 2481–2504. https://doi.org/10.1175/JAS-D-11-07.1

Maycock, A. C., & Hitchcock, P. (2015). Do split and displacement sudden stratospheric warmings have different annular mode signatures? *Geophysical Research Letters*, *42*(24), 10,943-10,951. https://doi.org/10.1002/2015GL066754

Met Office. (2018). *Snow and low temperatures February to March 2018*. Retrieved from https://www.metoffice.gov.uk/binaries/content/assets/metofficegovuk/pdf/weather/learn-about/uk-past-events/interesting/2018/snow-and-low-temperatures-february-to-march-2018---met-office.pdf

Mitchell, D. M., Gray, L. J., Anstey, J., Baldwin, M. P., & Charlton-Perez, A. J. (2013). The Influence of Stratospheric Vortex Displacements and Splits on Surface Climate. *Journal of Climate*, *26*(8), 2668–2682. https://doi.org/10.1175/JCLI-D-12-00030.1

Palmeiro, F. M., Iza, M., Barriopedro, D., Calvo, N., & García-Herrera, R. (2017). The complex behavior of El Niño winter 2015-2016. *Geophysical Research Letters*, *44*(6), 2902–2910. https://doi.org/10.1002/2017GL072920

Polvani, L. M., Sun, L., Butler, A. H., Richter, J. H., & Deser, C. (2017). Distinguishing Stratospheric Sudden Warmings from ENSO as Key Drivers of Wintertime Climate Variability over the North Atlantic and Eurasia. *Journal of Climate*, *30*, 1959–1969. https://doi.org/10.1175/JCLI-D-16-0277.s1

Polvani, L. M., & Waugh, D. W. (2004). Upward Wave Activity Flux as a Precursor to Extreme Stratospheric Events and Subsequent Anomalous Surface Weather Regimes. *Journal of Climate*, *17*(18), 3548–3554. https://doi.org/10.1175/1520-0442(2004)017<3548:UWAFAA>2.0.CO;2

Scaife, A. A., Folland, C. K., Alexander, L. V., Moberg, A., & Knight, J. R. (2008). European Climate Extremes and the North Atlantic Oscillation. *Journal of Climate*, *21*(1), 72–83. https://doi.org/10.1175/2007JCLI1631.1

Scaife, A. A., Karpechko, A. Y., Baldwin, M. P., Brookshaw, A., Butler, A. H., Eade, R., … Smith, D. (2016). Seasonal winter forecasts and the stratosphere. *Atmospheric Science Letters*, *17*(1), 51–56. https://doi.org/10.1002/asl.598

van der Schrier, G., dan den Besselaar, E. J. M., Klein Tank, A. M. G., & Verver, G. (2013). Monitoring European average temperature based on the E-OBS gridded data set. *J. Geophys. Res. Atmos*, *118*, 5120–5135. https://doi.org/10.1002/jgrd.50444

Tamarin-Brodsky, T., Hodges, K., Hoskins, B. J., & Shepherd, T. G. (2019). A Dynamical Perspective on Atmospheric Temperature Variability and its Response to Climate Change. *Journal of Climate*, JCLI-D-18-0462.1. https://doi.org/10.1175/JCLI-D-18-0462.1

Thompson, D. W. J., Baldwin, M. P., & Wallace, J. M. (2002). Stratospheric Connection to Northern Hemisphere Wintertime Weather: Implications for Prediction. *Journal of Climate*, *15*(12), 1421–1428. https://doi.org/10.1175/1520-0442(2002)015<1421:SCTNHW>2.0.CO;2

Tomassini, L., Gerber, E. P., Baldwin, M. P., Bunzel, F., & Giorgetta, M. (2012). The role of stratosphere-troposphere coupling in the occurrence of extreme winter cold spells over northern Europe. *Journal of Advances in Modeling Earth Systems*, *4*(4), n/a-n/a. https://doi.org/10.1029/2012MS000177

Trigo, R., Osborn, T., & Corte-Real, J. (2002). The North Atlantic Oscillation influence on Europe: climate impacts and associated physical mechanisms. *Climate Research*, *20*(1), 9–17. https://doi.org/10.3354/cr020009

Tripathi, O. P., Baldwin, M., Charlton-Perez, A., Charron, M., Eckermann, S. D., Gerber, E., … Son, S.-W. (2015). The predictability of the extratropical stratosphere on monthly time-scales and its impact on the skill of tropospheric forecasts. *Quarterly Journal of the Royal Meteorological Society*, *141*(689), 987–1003. https://doi.org/10.1002/qj.2432

Uppala, S. M., KÅllberg, P. W., Simmons, A. J., Andrae, U., Bechtold, V. D. C., Fiorino, M., … Woollen, J. (2005). The ERA-40 re-analysis. *Quarterly Journal of the Royal Meteorological Society*, *131*(612), 2961–3012. https://doi.org/10.1256/qj.04.176

Vautard, R., Gobiet, A., Sobolowski, S., Kjellström, E., Stegehuis, A., Watkiss, P., … Jacob, D. (2014). The European climate under a 2 °C global warming. *Environmental Research Letters*, *9*(3), 034006. https://doi.org/10.1088/1748-9326/9/3/034006

Whan, K., Zwiers, F., & Sillmann, J. (2016). The Influence of Atmospheric Blocking on Extreme Winter Minimum Temperatures in North America. *Journal of Climate*, *29*(12), 4361–4381. https://doi.org/10.1175/JCLI-D-15-0493.1

White, I., Garfinkel, C. I., Gerber, E. P., Jucker, M., Aquila, V., & Oman, L. D. (2019). The

Downward Influence of Sudden Stratospheric Warmings: Association with Tropospheric Precursors. *Journal of Climate*, *32*(1), 85–108. https://doi.org/10.1175/JCLI-D-18-0053.1

Woollings, T., Charlton-Perez, A., Ineson, S., Marshall, A. G., & Masato, G. (2010). Associations between stratospheric variability and tropospheric blocking. *Journal of Geophysical Research*, *115*(D6), D06108. https://doi.org/10.1029/2009JD012742

Zhang, X., Alexander, L., Hegerl, G. C., Jones, P., Tank, A. K., Peterson, T. C., … Zwiers, F. W. (2011). Indices for monitoring changes in extremes based on daily temperature and precipitation data. *Wiley Interdisciplinary Reviews: Climate Change*, *2*(6), 851–870. https://doi.org/10.1002/wcc.147

Figures and Tables

Table 1: Dates of SSW events used in this analysis based on the compendium compiled by Butler et al., (2017) from ERA-Interim data (Dee et al., 2011). Events marked in italics were winters when an SSW event occurred in March only and these were discounted in a sensitivity test. The SSW classification as "split" (S) or "displacement" (D) follows that used by Lehtonen & Karpechko, (2016) with the 2013 event classified using the results of Coy & Pawson, (2015). The SSW of February 2018 was not used in generating the climatology but was analysed separately (Figures 9, 10). The 2018 SSW central date is from Karpechko et al., (2018).

Event number	Date of SSW event	SSW classification
1	22nd February 1979	S
2	29th February 1980	D
3	*4th March 1981*	*D*
4	4th December 1981	D
5	24th February 1984	D
6	1st January 1985	S
7	23rd January 1987	D
8	8th December 1987	S
9	14th March 1988	S
10	21st February 1989	S
11	15th December 1998	D

12	26th February 1999	S
13	*20th March 2000*	*D*
14	11th February 2001	S
15	30th December 2001	D
16	18th January 2003	S
17	5th January 2004	D
18	21st January 2006	D
19	24th February 2007	D
20	22nd February 2008	D
21	24th January 2009	S
22	9th February 2010	S
23	24th March 2010	D
24	6th January 2013	S
-	12th February 2018	-

Table 2: Mean and extreme indices calculated from E-OBS data and used in this analysis.

Index	**Definition**
TN	Average minimum temperature
TX	Average maximum temperature
TNn	Lowest daily minimum temperature per winter/per 30-day period
TXn	Lowest daily maximum temperature per winter/per 30-day period

RR	Average precipitation total
Rx1day	Highest daily precipitation per winter/per 30-day period
WD	Number of wet days (precipitation > 1mm)

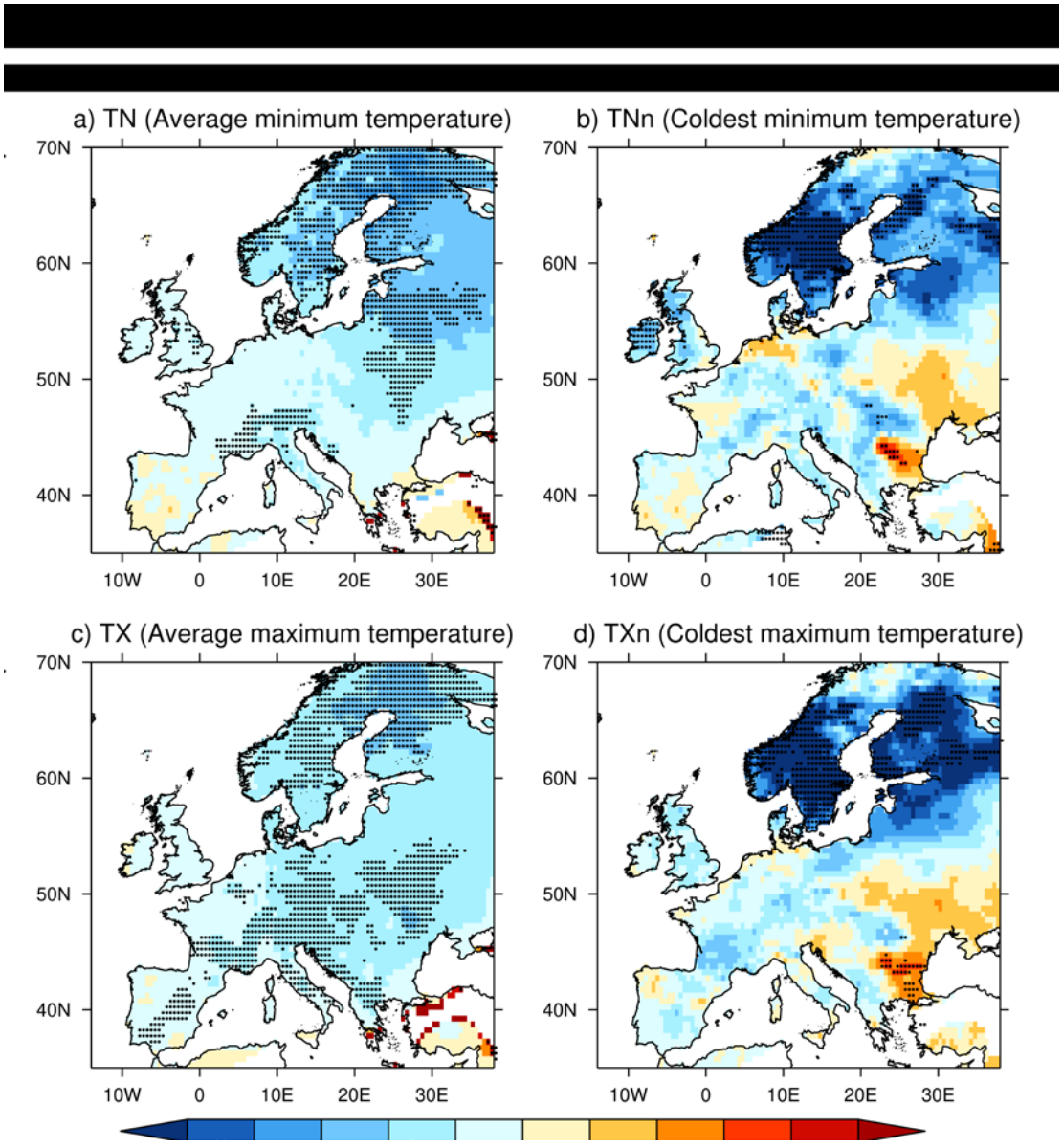

Figure 1: Average difference in cold season (Nov-Apr) a) average minimum temperature, b) coldest minimum temperature, c) average maximum temperature, and d) coldest maximum temperature between seasons with SSWs and seasons without SSWs. Stippling indicates median-averages are significantly different at the 5% level as measured by a Wilcoxon rank-sum test. The boxes in a) show the four regions used for regional-average analysis. Land regions in white are missing data.

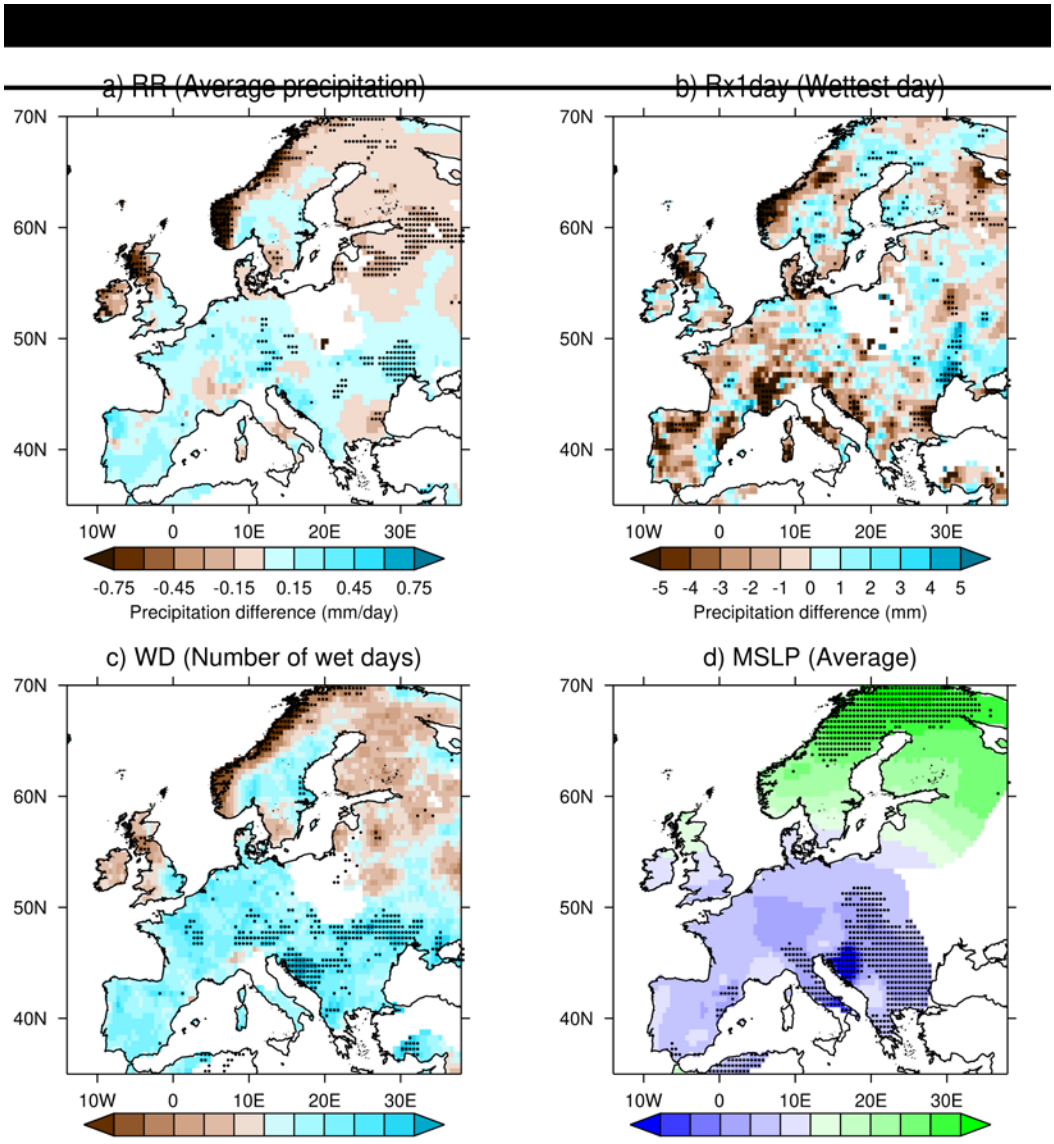

Figure 2: Average difference in cold season (Nov-Apr) a) average precipitation, b) maximum daily precipitation, c) number of wet days (>1mm of precipitation), and d) mean sea level pressure between seasons with SSWs and seasons without SSWs. Stippling indicates median-averages are significantly different at the 5% level as measured by a Wilcoxon rank-sum test.

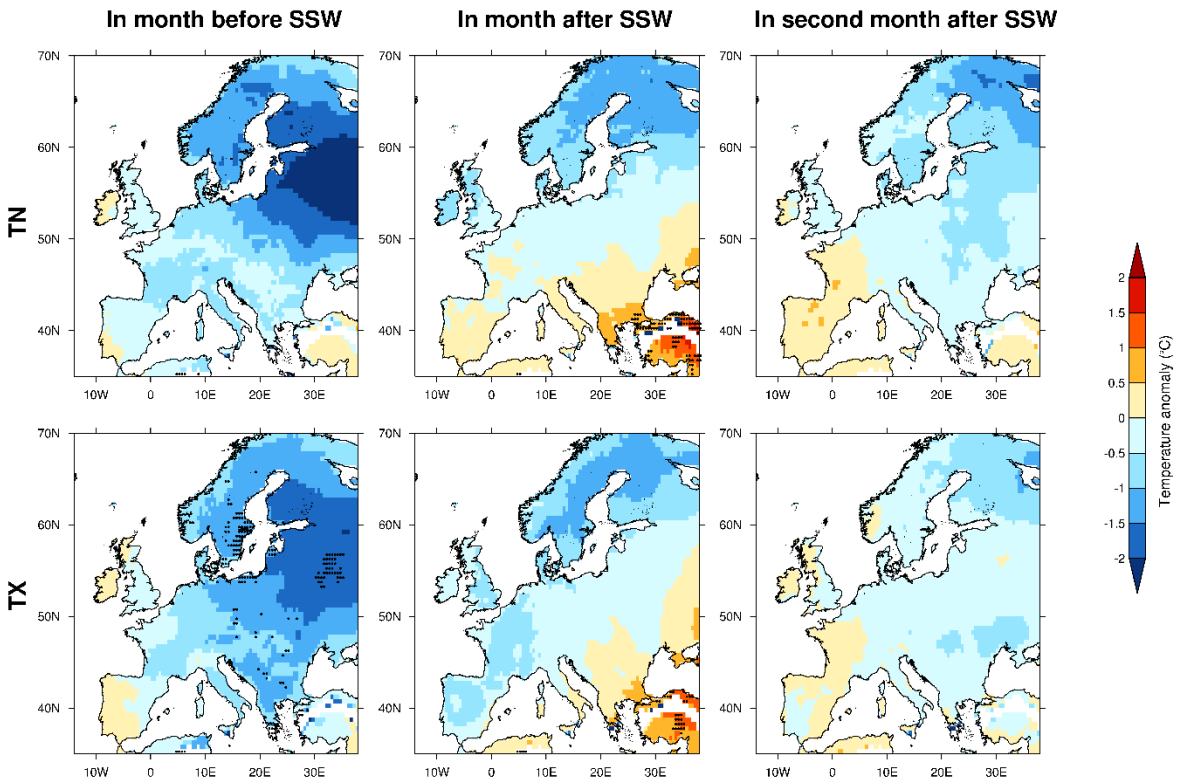

Figure 3: Monthly-average daily minimum (top row) and maximum temperature anomalies (bottom row) before and after central dates of SSW events. Stippling indicates at least 75% of gridbox anomalies across individual SSW events are of the same sign. Anomalies are calculated from a daily climatological average for 1979-2016 to remove the influence of the seasonal cycle.

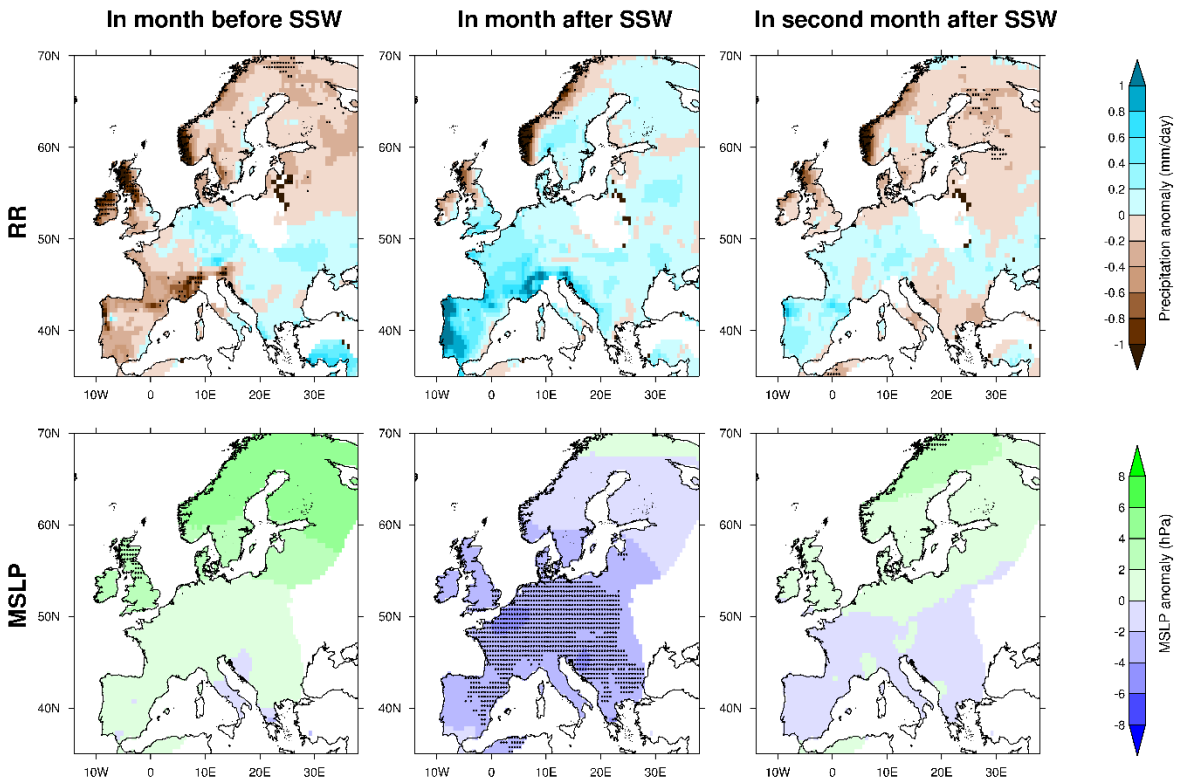

Figure 4: Monthly-average precipitation (top row) and mean sea level pressure anomalies (bottom row) before and after central dates of SSW events. Stippling indicates at least 75% of gridbox anomalies across individual SSW events are of the same sign. Anomalies are calculated from a daily climatological average for 1979-2016 to remove the influence of the seasonal cycle.

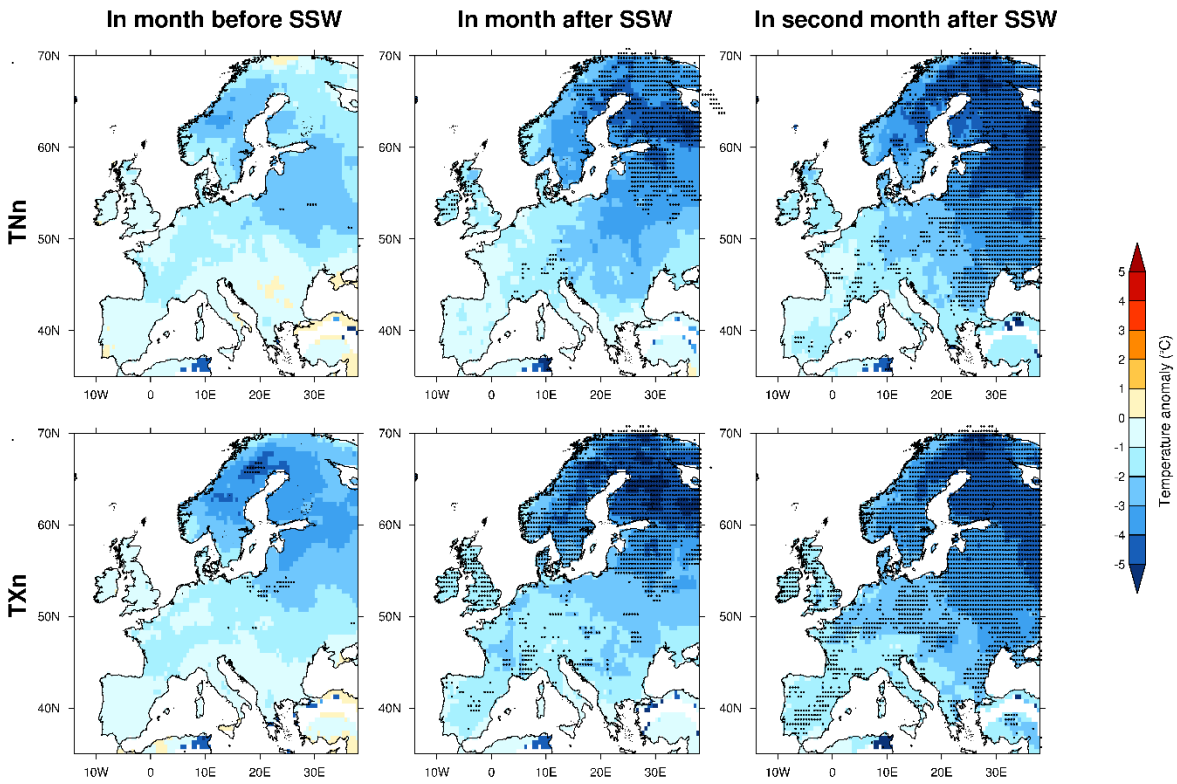

Figure 5: Average anomalous intensity of the coldest minimum (top row) and coldest maximum temperatures (bottom row) before and after central dates of SSW events. Stippling indicates at least 75% of gridbox anomalies across individual SSW events are of the same sign. Anomalies are calculated from a daily climatological average for 1979-2016 to remove the influence of the seasonal cycle.

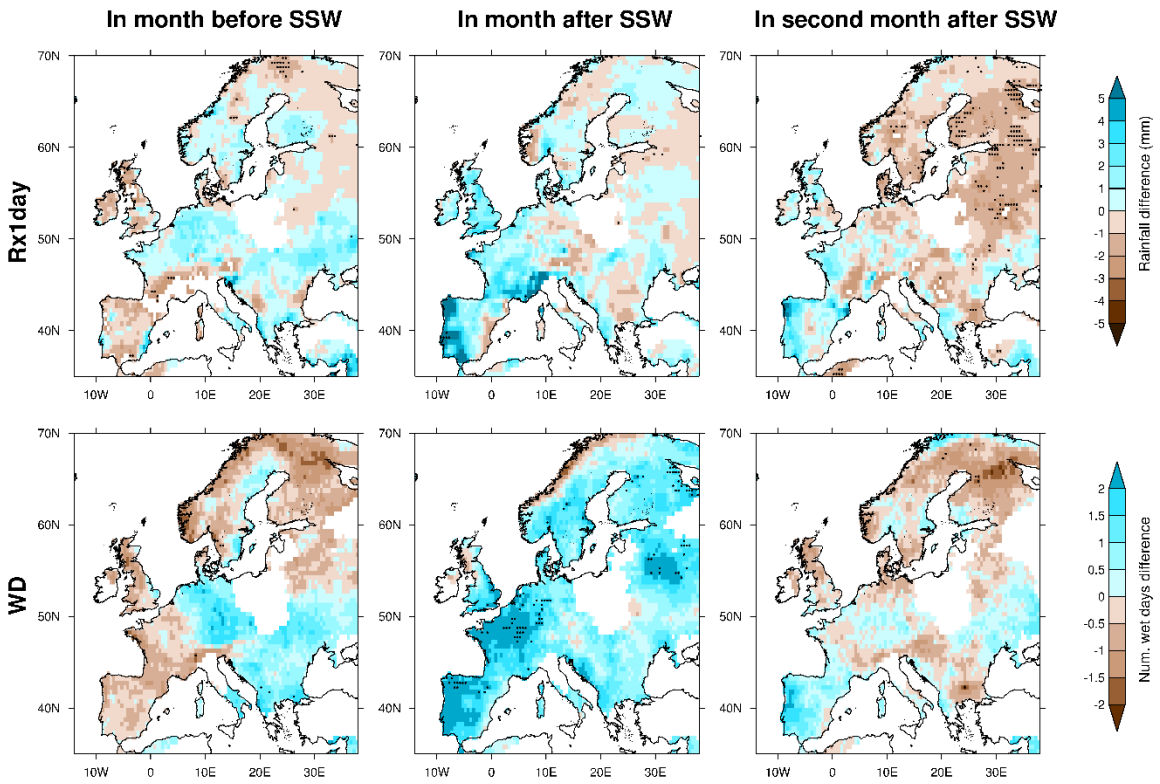

Figure 6: Anomalous intensity of the 1-day maximum precipitation (top row) and the number of wet days (bottom row) before and after central dates of SSW events. Stippling indicates at least 75% of gridbox anomalies across individual SSW events are of the same sign. Anomalies are calculated from a daily climatological average for 1979-2016 to remove the influence of the seasonal cycle.

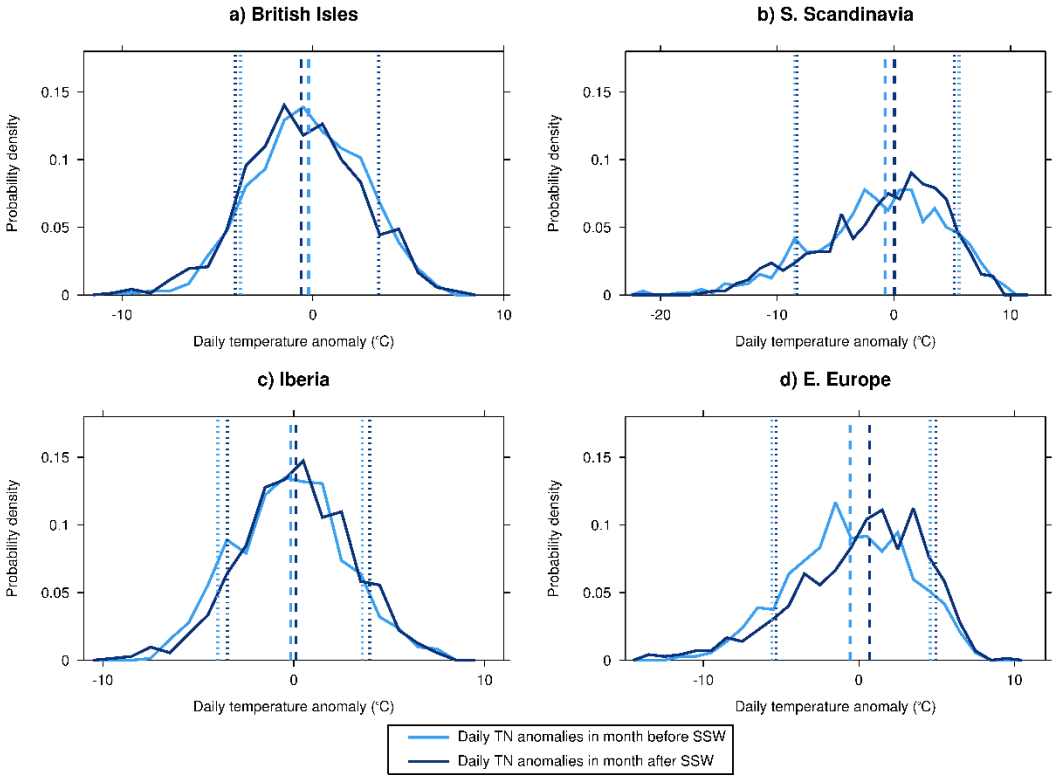

Figure 7: Probability density functions of daily area-average minimum temperatures in 30-day windows before SSW events (light blue) and 30-day windows after SSW events (dark blue) for a) the British Isles [11°W-2°E, 50°N-60°N], b) Southern Scandinavia [3°E-18°E, 57°N-64°N], c) Iberia [10°W-1°E, 36°N-44°N], and d) Eastern Europe [18°E-26°E, 40°N-50°N]. Only land-based gridboxes are calculated in E-OBS and used in calculating these area-averages. The dashed lines show the median-average daily minimum temperature anomalies before (light blue dashed) and after SSWs (dark blue dashed). The dotted lines show the 10th and 90th percentiles of daily minimum temperature anomalies before (light blue dotted) and after SSWs (dark blue dotted).

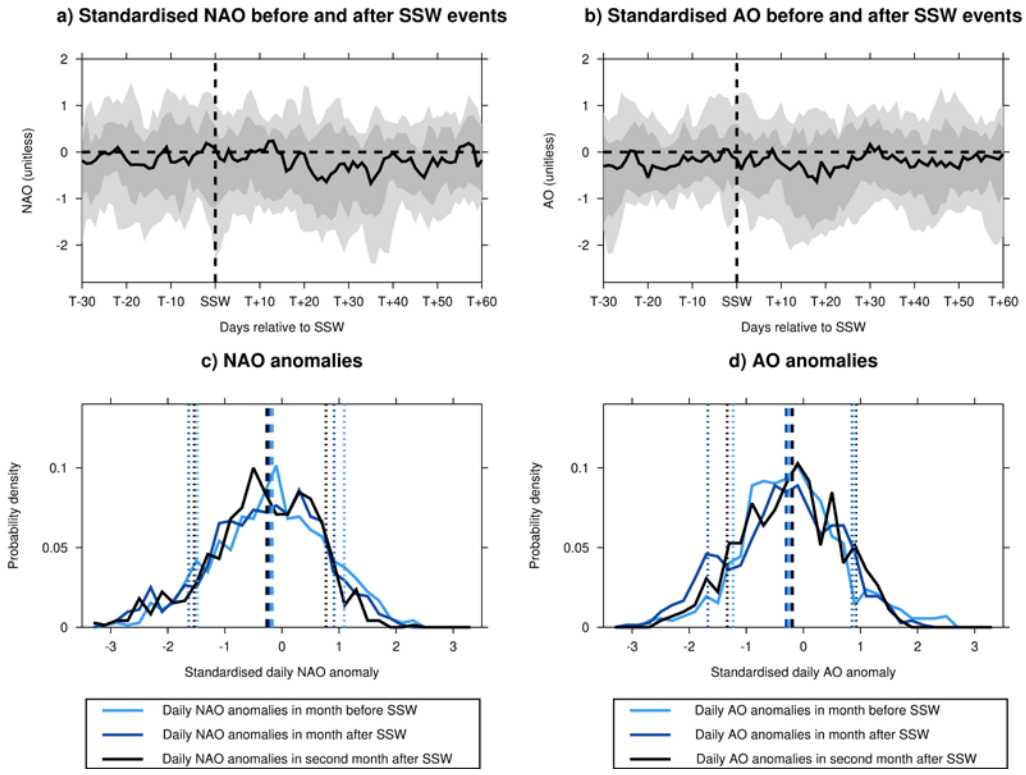

Figure 8: a), b) Daily-average standardised NAO and AO anomalies respectively before and after SSW events. Black line shows median anomalies with dark grey bars showing interquartile range and light grey bars showing 10^{th}-90^{th} percentile anomalies. c), d) Probability density functions of daily standardised NAO and AO anomalies respectively in 30-day windows before SSW events (light blue) and 30-day windows immediately after SSW events (dark blue) and the second month after SSW events (black). The dashed lines show the median-average daily NAO anomalies before (light blue dashed), immediately after (dark blue dashed), and in the second month after SSWs (black dashed). The dotted lines show the

10^{th} and 90^{th} percentiles of daily NAO anomalies before (light blue dotted), immediately after (dark blue dotted), and in the second month after SSWs (black dotted).

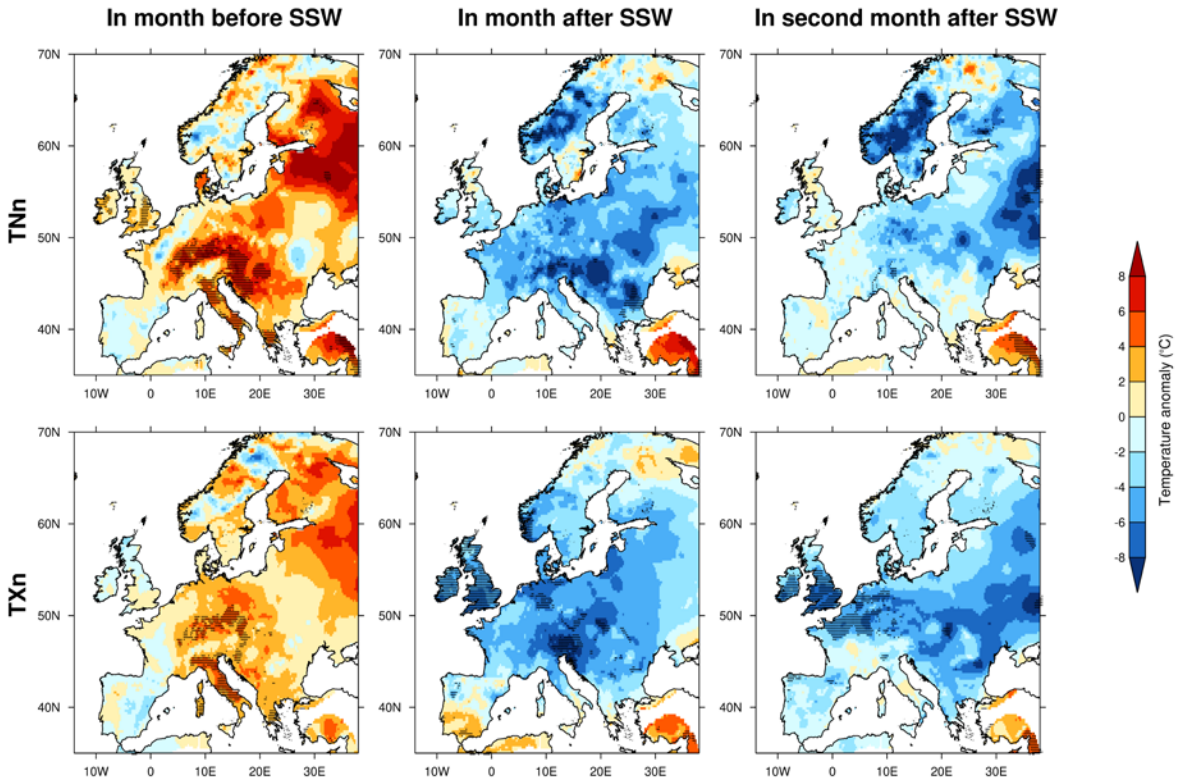

Figure 9: Anomalous intensity of the coldest minimum (top row) and coldest maximum temperatures (bottom row) before and after the central date of the SSW in 2018. Anomalies are calculated from a daily climatological average for 1979-2016 to remove the influence of the seasonal cycle. Stippling indicates that the anomaly in the coldest minimum or coldest maximum is record high or low relative to the equivalent anomalies of the 24 SSWs in the climatology.

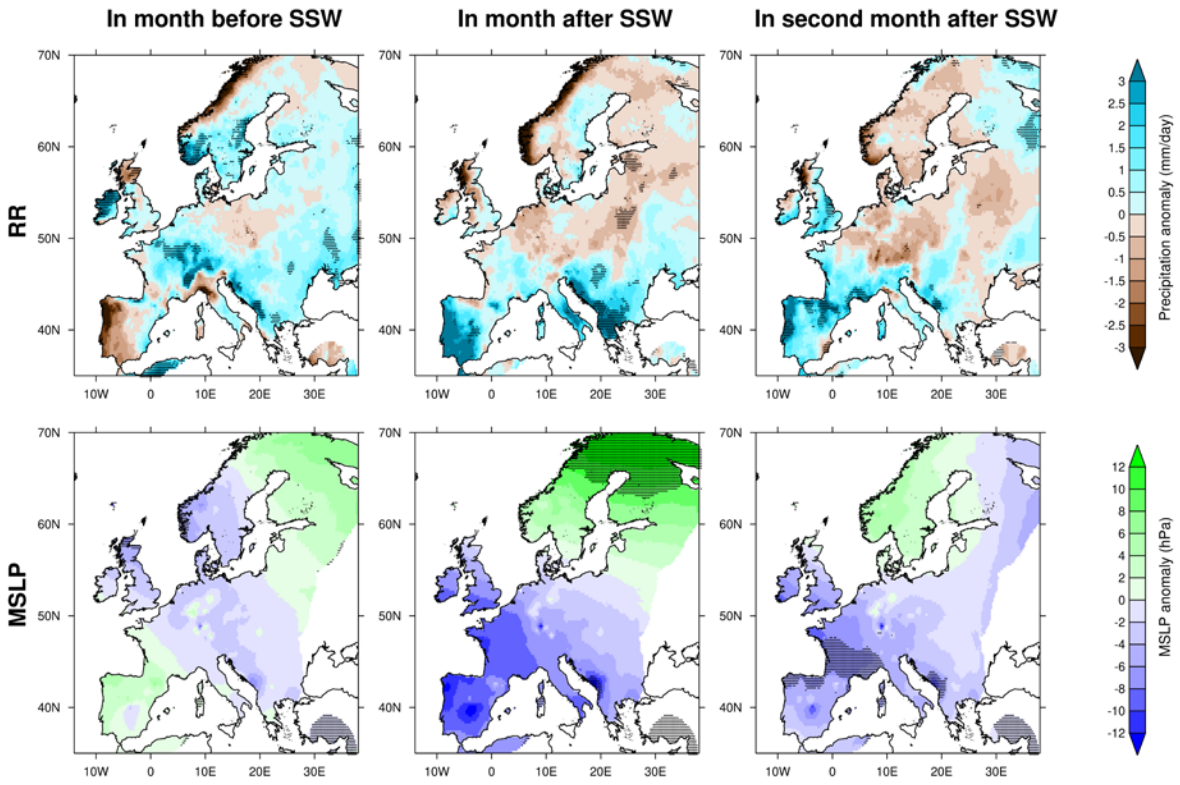

Figure 10: As Figure 9 but for average anomalies in 30-day precipitation and mean sea level pressure before and after the SSW of 2018.

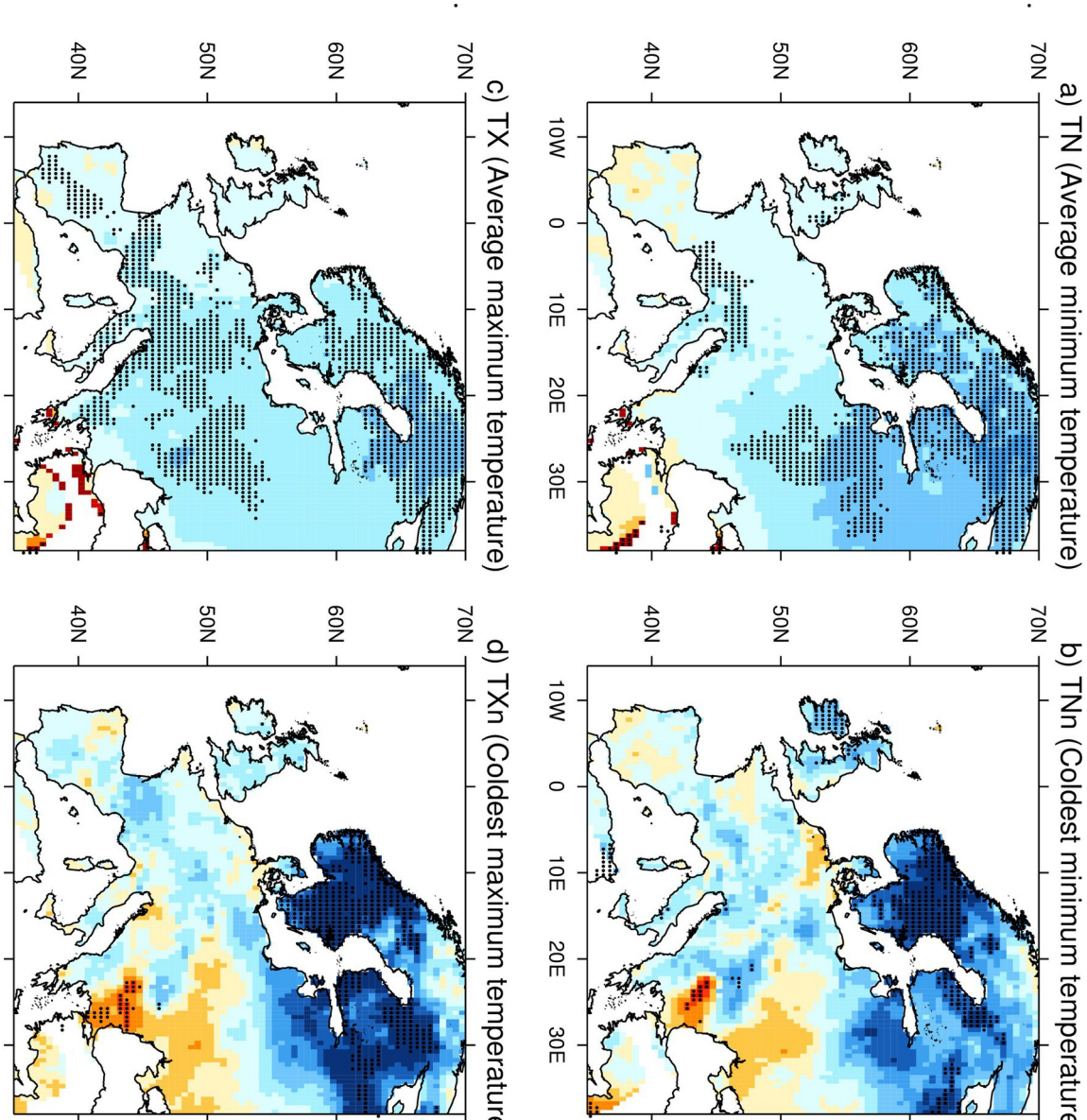

2019jd030480-f01-z-.eps

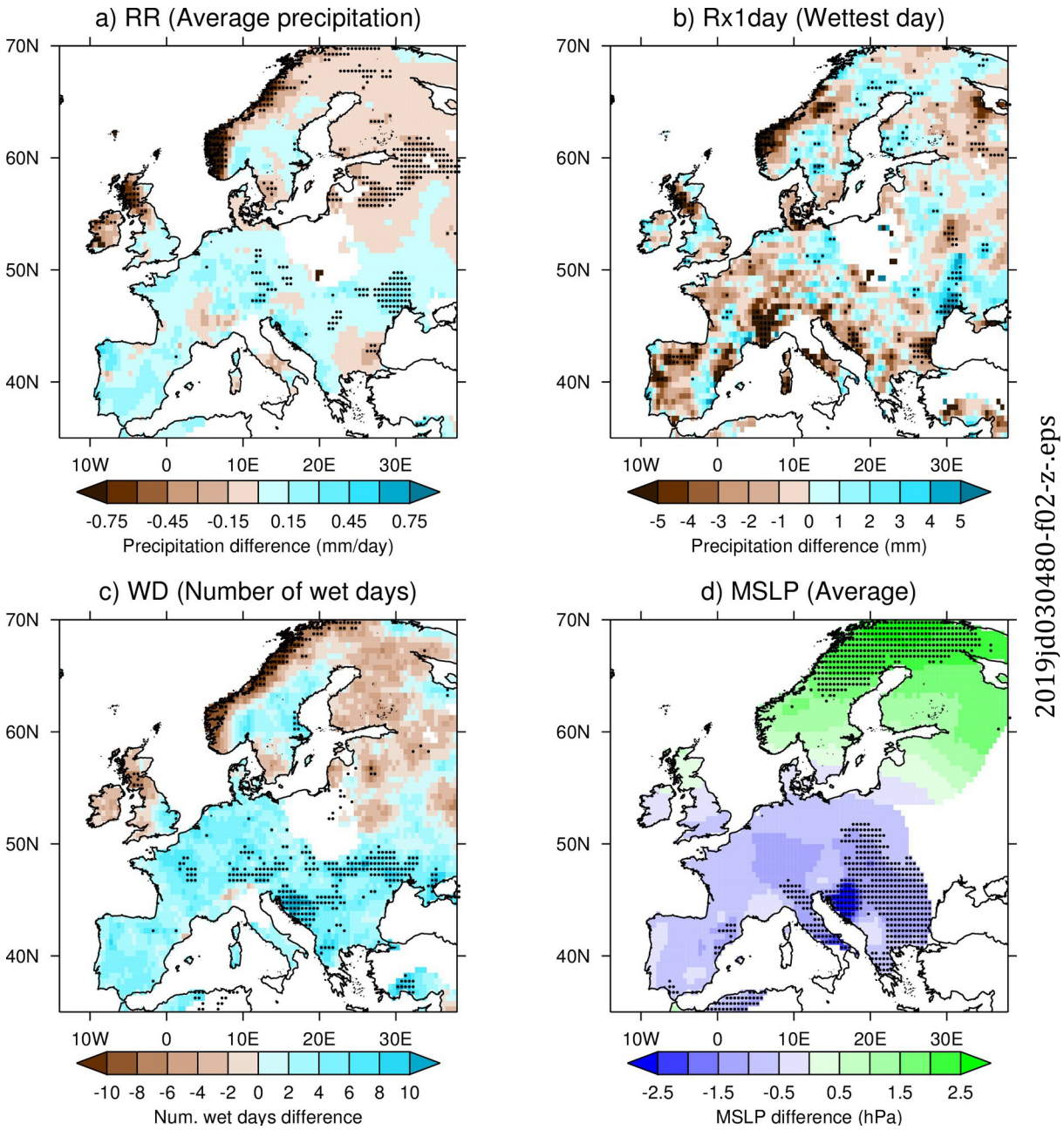

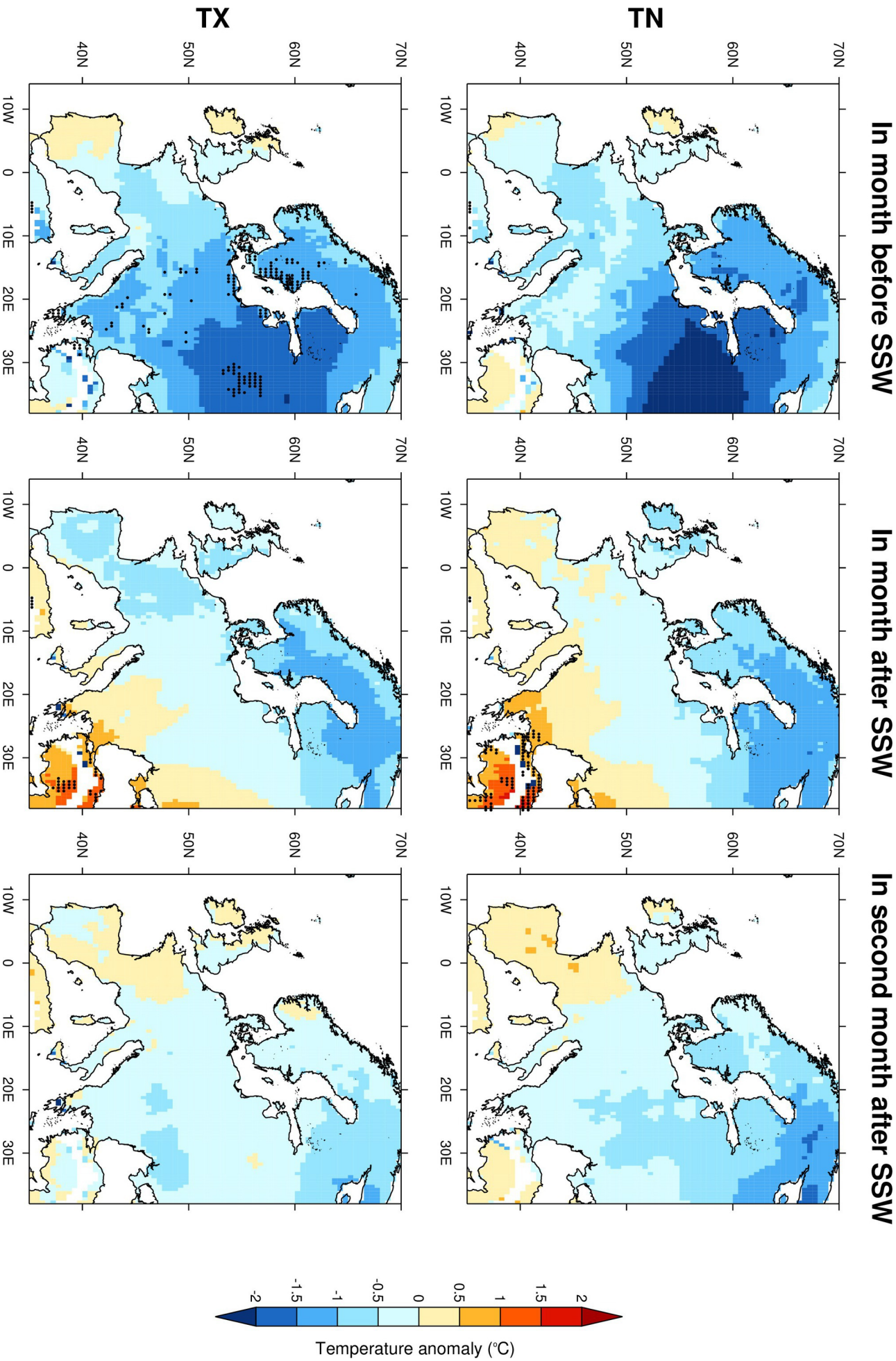

2019jd030480-f03-z-.eps

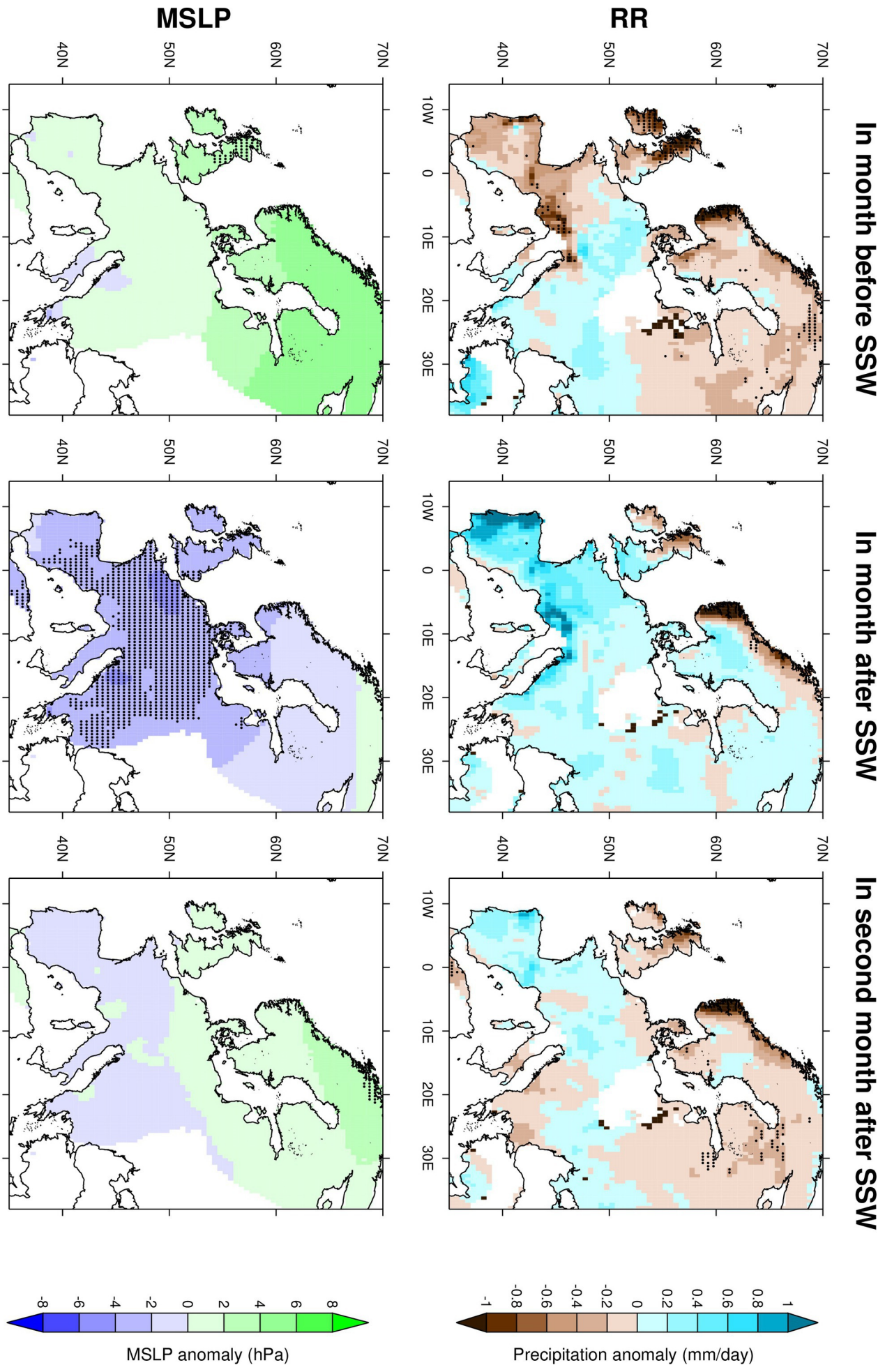

2019jd030480-f04-z-.eps

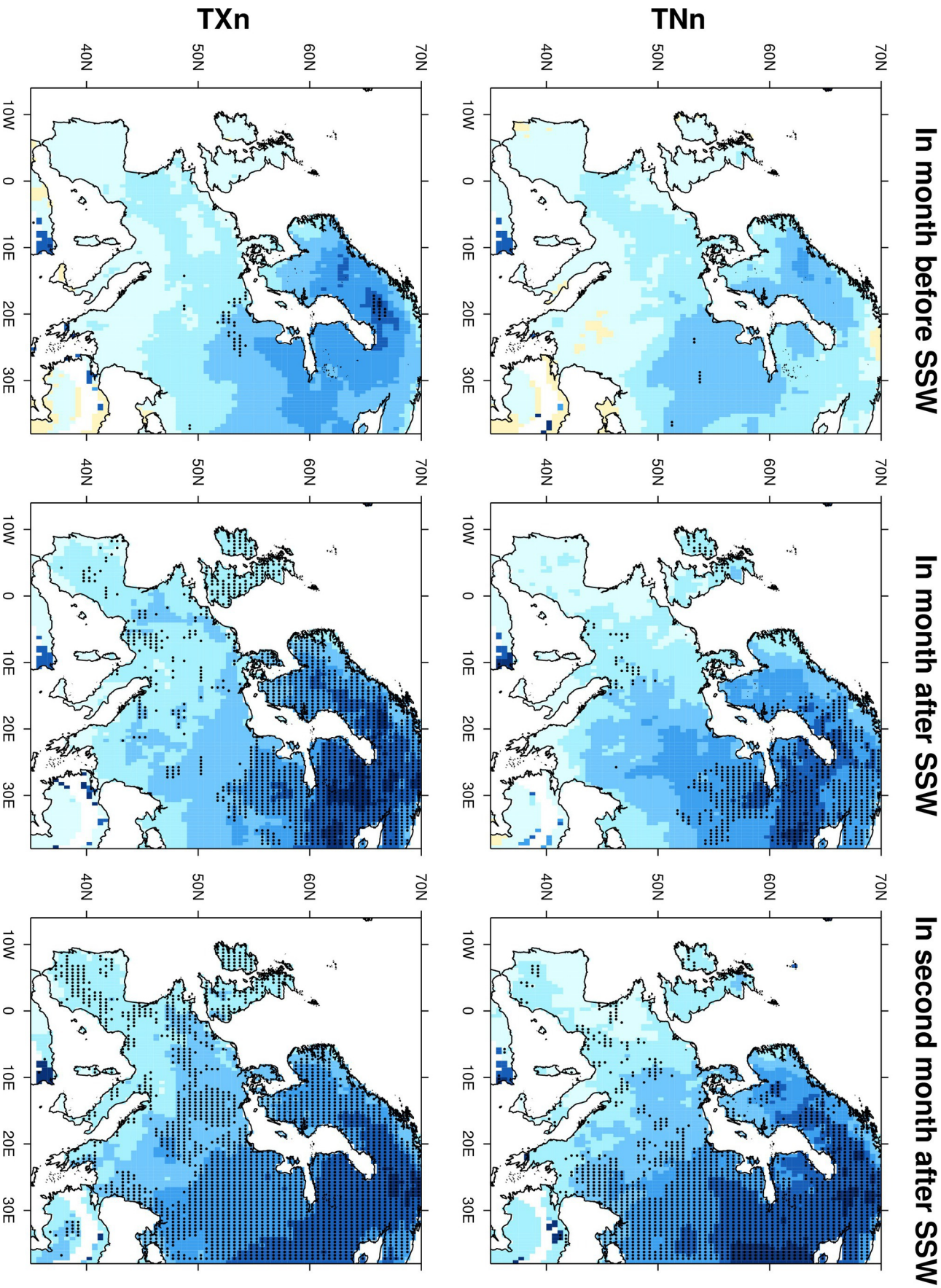

2019jd030480-f05-z-.eps

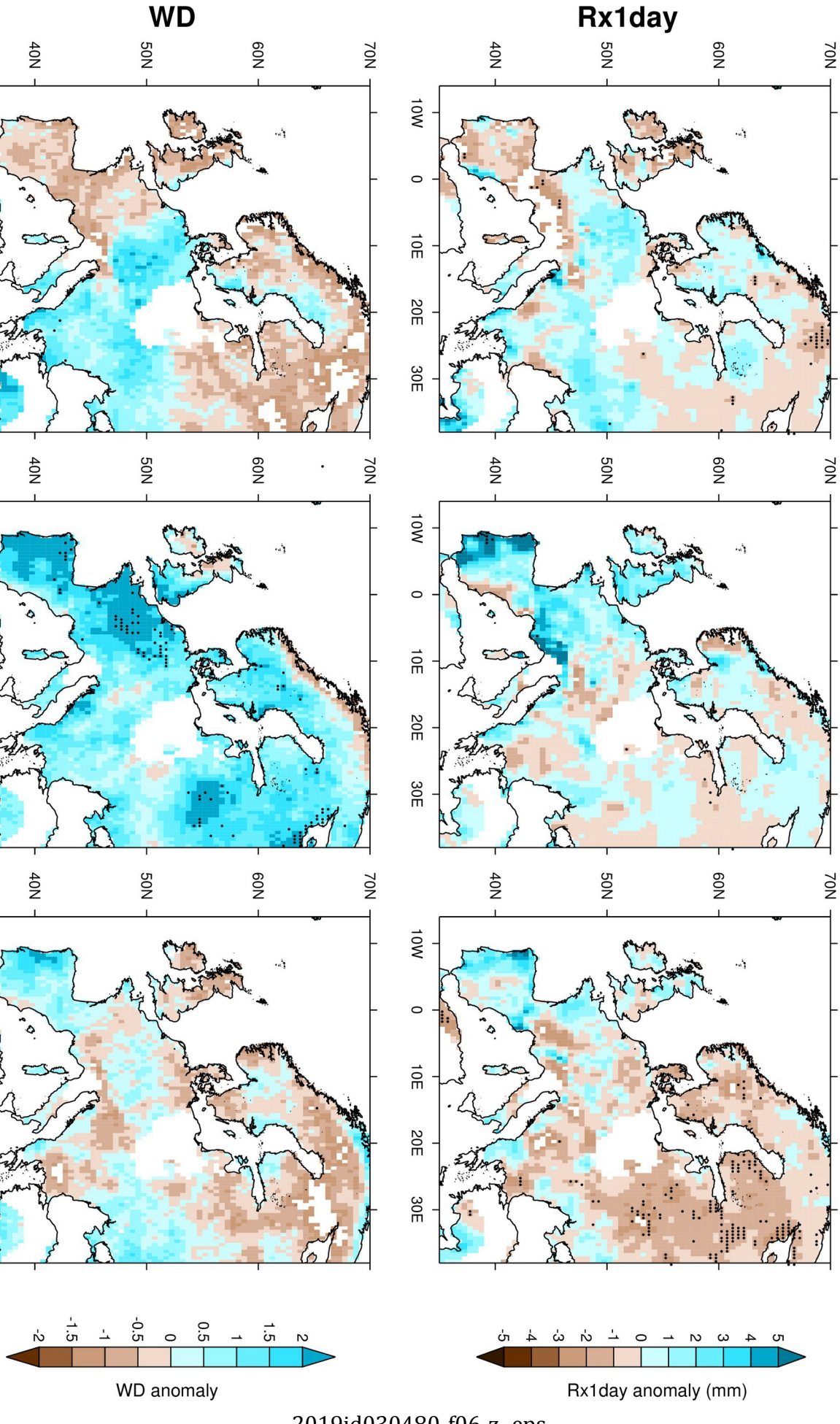

2019jd030480-f06-z-.eps

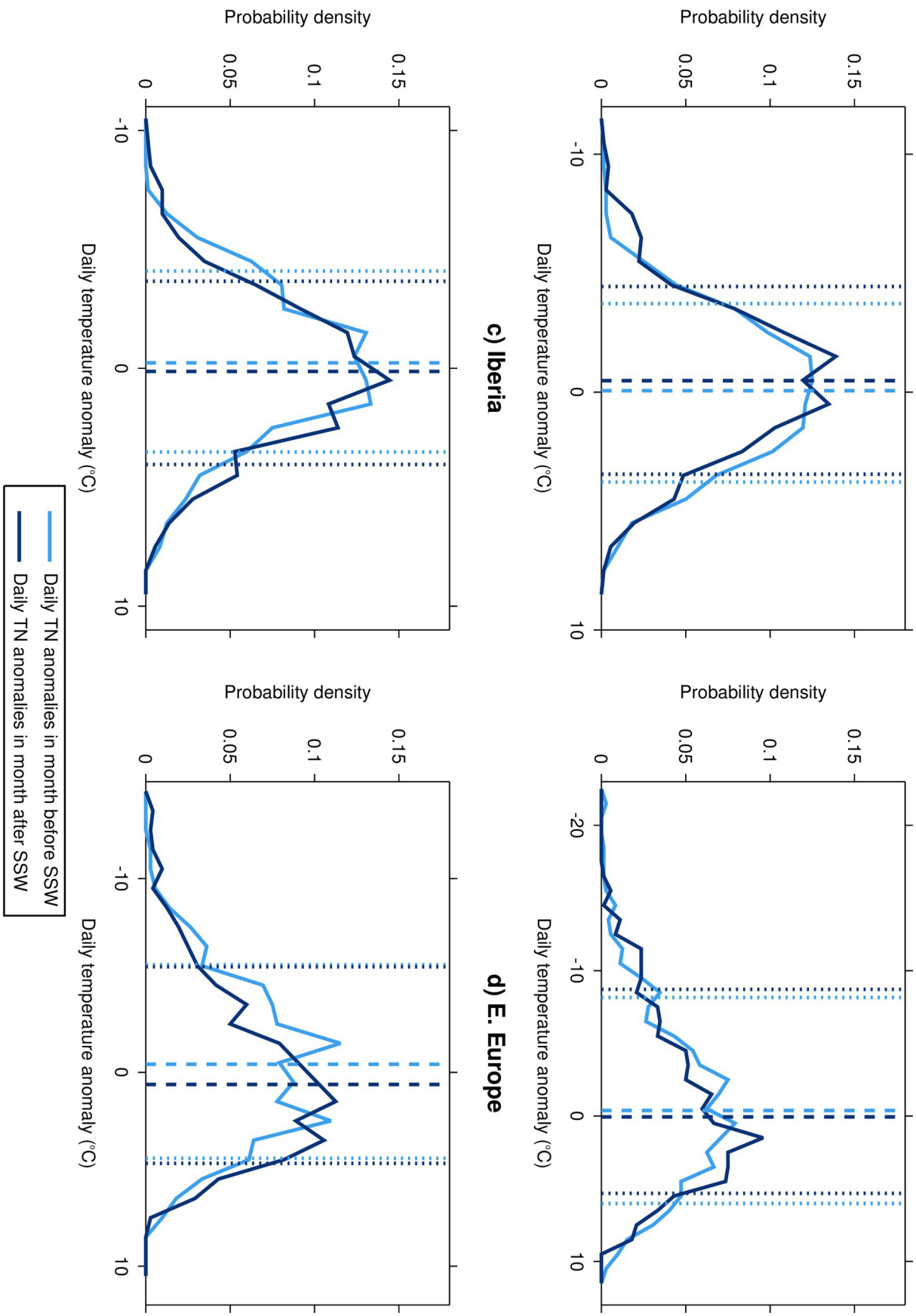

2019jd030480-f07-z-.eps

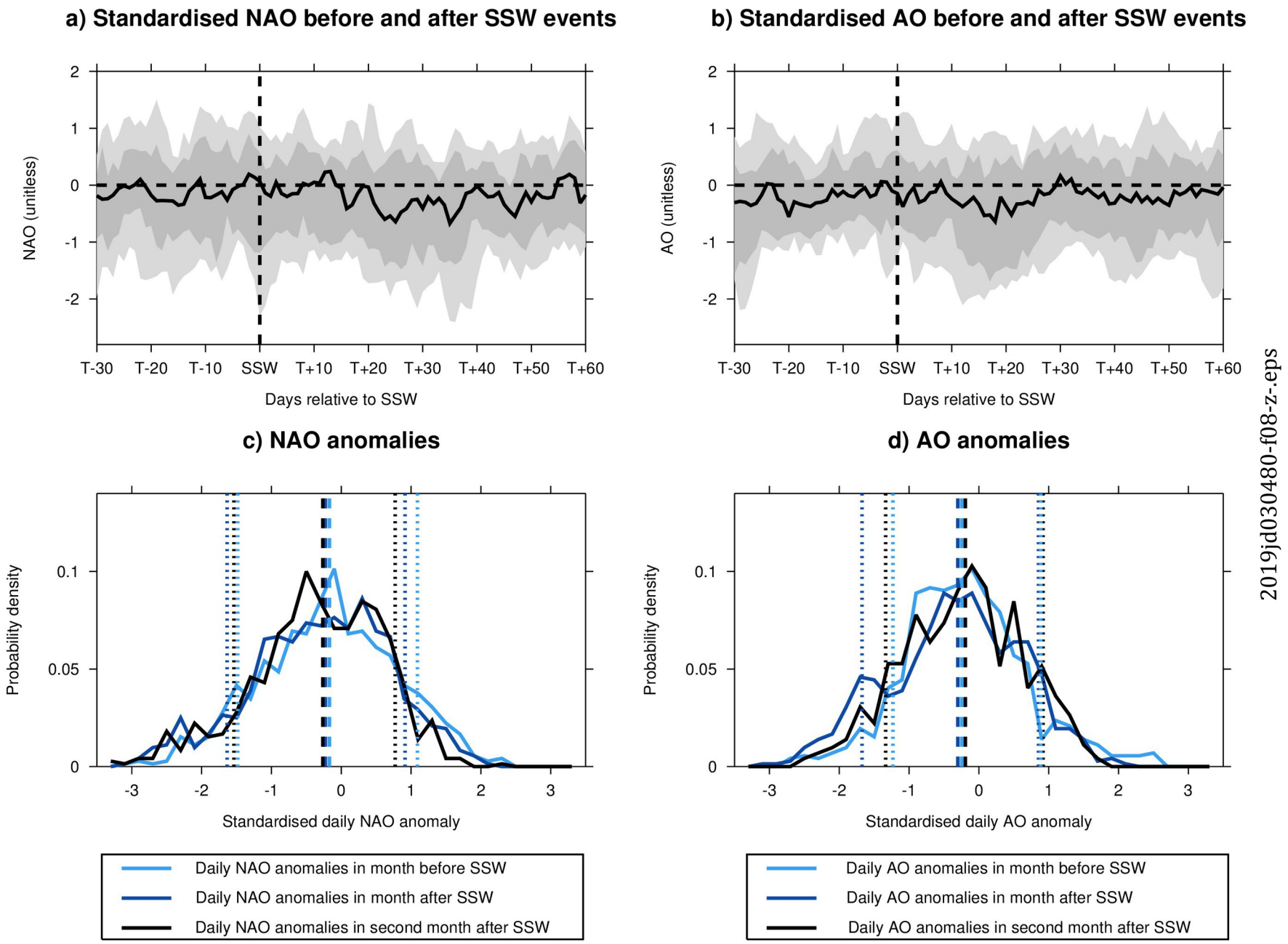

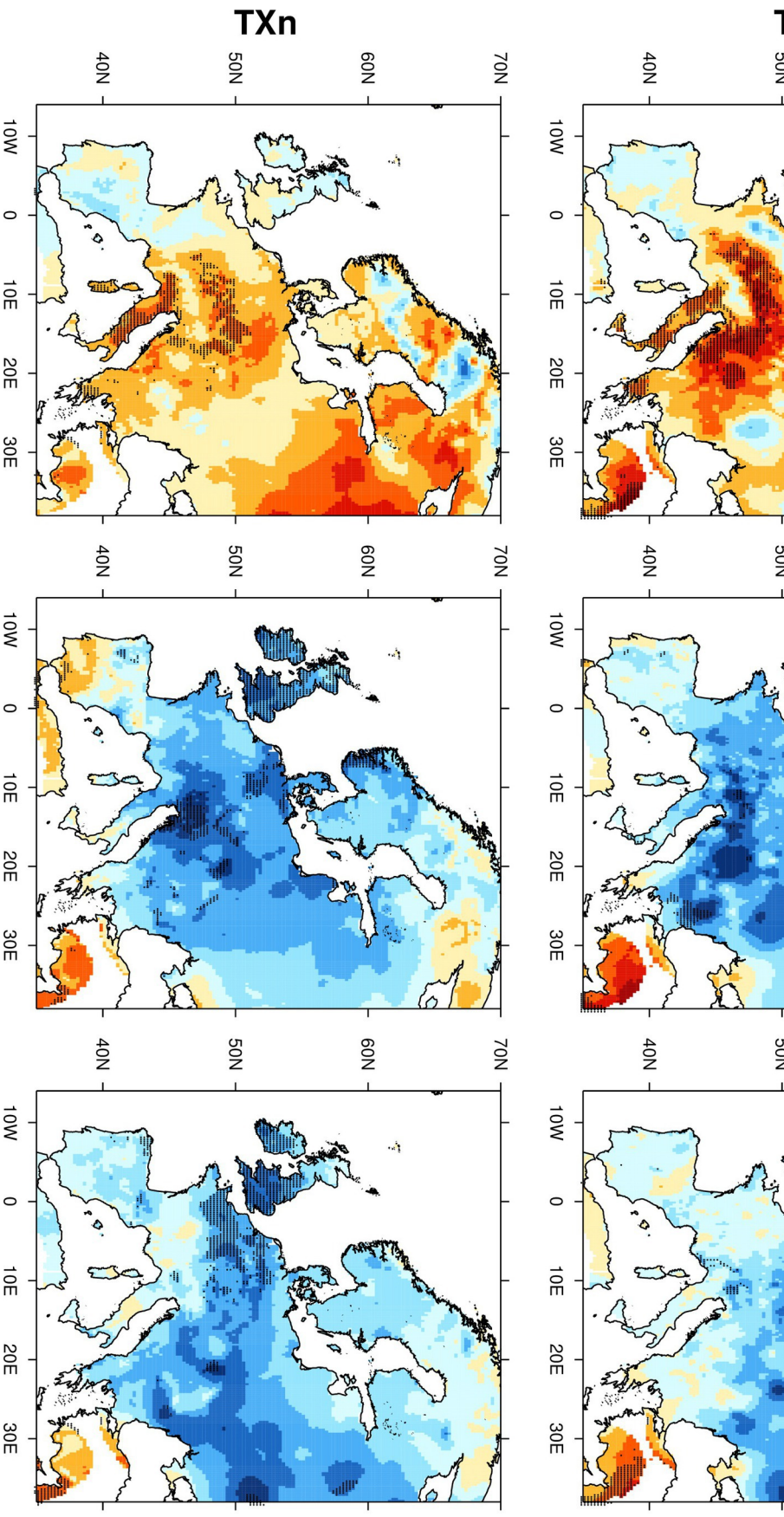

2019jd030480-f09-z-.eps

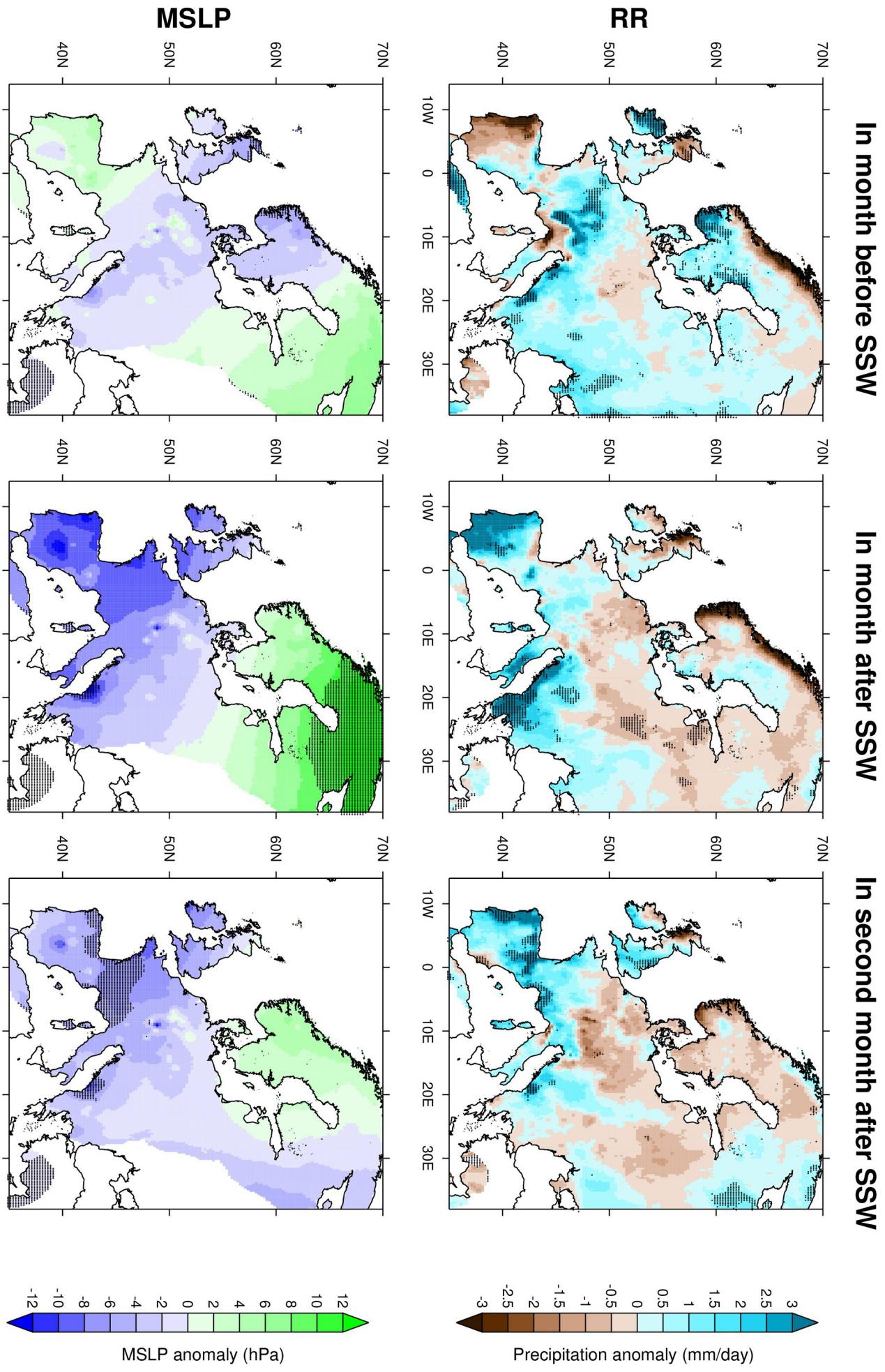

2019jd030480-f10-z-.eps